A histone H4 lysine 20 methyltransferase couples environmental cues
to sensory neuron control of developmental plasticity

Colin E Delaney[1], Albert T Chen[2], Jacqueline V Graniel[2],
Kathleen J Dumas[2,4], and Patrick J Hu[1,2,3,5,6]

Departments of [1]Cell and Developmental Biology and [2]Internal Medicine, and [3]Institute of Gerontology, University of Michigan Medical School, Ann Arbor, Michigan 48109
Present addresses: [4]Buck Institute for Research on Aging, Novato, California 94945;
[5]Departments of Medicine, Cell and Developmental Biology, and Cancer Biology, Vanderbilt University School of Medicine, Nashville, Tennessee 37232

[6]Corresponding author: patrick.j.hu@vanderbilt.edu

Keywords: *C. elegans,* dauer, dosage compensation, H4K20, insulin-like peptides, FoxO

SUMMARY STATEMENT

We describe a new role for the *C. elegans* histone methyltransferase SET-4 in linking environmental signals to diapause through regulation of the X-linked insulin-like peptide gene *ins-9* in sensory neurons
.

ABSTRACT

Animals change developmental fates in response to external cues. In the nematode *Caenorhabditis elegans*, unfavorable environmental conditions induce a state of diapause known as dauer by inhibiting the conserved DAF-2 insulin-like signaling (ILS) pathway through incompletely understood mechanisms. We previously established a role for the *C. elegans* dosage compensation protein DPY-21 in the control of dauer arrest and DAF-2 ILS. Here we show that the histone H4 lysine 20 methyltransferase SET-4, which also influences dosage compensation, promotes dauer arrest in part by repressing the X-linked *ins-9* gene, which encodes a new agonist insulin-like peptide (ILP) expressed specifically in the paired ASI sensory neurons that are required for dauer bypass. *ins-9* repression in dauer-constitutive mutants requires DPY-21, SET-4, and the FoxO transcription factor DAF-16, which is the main target of DAF-2 ILS. In contrast, autosomal genes encoding major agonist ILPs that promote reproductive development are not repressed by DPY-21, SET-4, or DAF-16/FoxO. Our results implicate SET-4 as a sensory rheostat that reinforces developmental fates in response to environmental cues by modulating autocrine and paracrine DAF-2 ILS.

INTRODUCTION

To maintain evolutionary fitness, organisms must react appropriately to environmental cues. The free-living nematode *Caenorhabditis elegans* has evolved a developmental strategy to optimize survival in changing environments. Under replete conditions, larvae progress through four stages (L1 – L4) to become reproductive adults. In adverse conditions such as overcrowding, heat, or food scarcity, larvae arrest in an alternative stage known as dauer. Adapted for survival in harsh environments, dauers are morphologically, metabolically, and behaviorally distinct from reproductive L3 larvae. Improvement of ambient conditions induces dauer exit and resumption of reproductive development (Fielenbach and Antebi, 2008; Riddle, 1988). The dominant environmental cue that influences dauer arrest is a constitutively elaborated pheromone that indicates population density (Butcher et al., 2008; Golden and Riddle, 1982).

C. elegans dauer arrest has served as a useful paradigm for understanding the molecular basis for developmental plasticity. Genetic analysis has defined four conserved signaling pathways that promote reproductive development in favorable environments. The DAF-11 transmembrane guanylyl cyclase acts in chemosensory neurons to regulate dauer arrest through the cyclic nucleotide-gated channel subunits TAX-2 and TAX-4. Downstream of DAF-11, DAF-2 insulin receptor (InsR) and DAF-7 transforming growth factor-β (TGFβ)-like pathways act in parallel to promote reproductive development by inhibiting the activities of the FoxO transcription factor DAF-16 and the SMAD transcription factor DAF-3, respectively. Distal to DAF-16/FoxO and DAF-3/SMAD, bile-acid-like steroid hormones known as dafachronic acids (DAs) promote reproductive development by regulating the activity of the conserved nuclear receptor DAF-12 (Fielenbach and Antebi, 2008).

While genetic analysis has identified how components of the DAF-11, DAF-2/InsR, DAF-7/TGFβ, and DAF-12 pathways interact to promote reproductive development in favorable conditions (Gottlieb and Ruvkun, 1994; Riddle et al., 1981; Thomas et al., 1993; Vowels and Thomas, 1992), the molecular nature of the upstream events that couple external cues to the activities of these pathways remains poorly understood. Laser ablation experiments demonstrated that the amphid sensory neurons are required for induction of dauer arrest by pheromone (Schackwitz et al., 1996; Vowels and Thomas, 1994). Indeed, the dauer-inhibitory ASI sensory neurons (Bargmann and Horvitz, 1991) are specific sites of expression of three insulin-like peptides (ILPs) that promote reproductive development

through DAF-2/InsR (INS-4, INS-6, and DAF-28) (Chen and Baugh, 2014; Cornils et al., 2011; Hung et al., 2014; Li et al., 2003) as well as the DAF-7 TGFβ-like ligand that promotes reproductive development (Ren et al., 1996; Schackwitz et al., 1996). Furthermore, crude dauer pheromone reduces the expression of DAF-28 and DAF-7 in ASI (Li et al., 2003; Schackwitz et al., 1996), suggesting that pheromone induces dauer arrest at least in part by reducing the expression of agonist ligands in sensory neurons that regulate DAF-2/InsR and TGFβ-like signaling. How pheromone represses these ligands remains a mystery.

We previously reported an unforeseen role for the *C. elegans* dosage compensation protein DPY-21 in promoting dauer arrest through inhibition of the DAF-2/InsR pathway (Dumas et al., 2013). DPY-21 is a component of the condensin-like dosage compensation complex (DCC) that equalizes X-linked gene expression between males and hermaphrodites by binding to both hermaphrodite X chromosomes during embryogenesis and repressing gene expression approximately two-fold (Meyer, 2010; Yonker and Meyer, 2003). Here we show that the conserved histone H4 lysine 20 (H4K20) methyltransferase SET-4, which also influences dosage compensation (Kramer et al., 2015; Vielle et al., 2012; Wells et al., 2012), promotes dauer arrest in a sex-specific manner by synergizing with DAF-16/FoxO to repress *ins-9,* an X-linked gene that encodes an ILP expressed specifically in ASI neurons (Chen and Baugh, 2014; Pierce et al., 2001). These findings reveal a sexually dimorphic role for regulators of histone H4K20 methylation in broadening the dynamic range of sensory responses to environmental cues that control developmental plasticity.

RESULTS

SET-4 acts through DAF-2 ILS to promote dauer arrest in a sex-specific manner

DAF-2/InsR promotes reproductive development by activating a conserved phosphoinositide 3-kinase (PI3K)/Akt pathway to inhibit DAF-16/FoxO (Murphy and Hu, 2013). The conserved protein EAK-7 acts in parallel to AKT-1 to inhibit nuclear DAF-16/FoxO activity (Alam et al., 2010). In contrast to *eak-7* and *akt-1* single mutants, which develop reproductively, *eak-7;akt-1* double mutant animals arrest as dauers in a DAF-16/FoxO-dependent manner (Alam et al., 2010). To identify new DAF-16/FoxO regulators, we performed a forward genetic screen for *s*uppressors of the *eak-7;akt-1* dauer-constitutive phenotype (*seak*). The first *seak* mutants characterized harbored loss-of-function mutations in the dosage compensation gene *dpy-21* (Dumas et al., 2013)*. dpy-21* encodes a conserved component of the condensin-like dosage compensation complex (DCC) that binds to X chromosomes and represses X-linked gene expression (Meyer, 2010; Yonker and Meyer, 2003). One *seak* mutant strain contained a point mutation in *set-4*, which encodes a histone H4K20 methyltransferase homolog that influences dosage compensation (Vielle et al., 2012; Wells et al., 2012). *set-4(dp268)* is predicted to change the conserved SET domain catalytic residue serine 182 (Southall et al., 2014) to phenylalanine (Figure 1A, Figure S1A). In light of our findings on *dpy-21* (Dumas et al., 2013)*,* we tested the possibility that *set-4(dp268)* was the causative *seak* mutation in this strain. After outcrossing removed all but two closely linked single nucleotide variants, *set-4(dp268)* suppressed dauer arrest to a similar extent as two independently derived *set-4* deletions, *n4600* (Andersen and Horvitz, 2007) and *ok1481* (Figure 1B)*.* Furthermore, an integrated single-copy *HA::set-4* transgene rescued dauer arrest in *set-4(n4600)* animals (Figure 1C and S1B). Therefore, SET-4 promotes dauer arrest.

DPY-21 enhances dauer arrest by activating DAF-16/FoxO, indicating that it acts in the DAF-2/InsR pathway to regulate dauer formation (Dumas et al., 2013). To determine whether SET-4 functions in the DAF-2/InsR pathway, we tested the effect of *set-4* mutation on dauer-constitutive phenotypes caused by mutations in the *daf-2/InsR, daf-7/TGFβ,* and *daf-12* pathways. *set-4* mutation suppressed the dauer-constitutive phenotypes of *daf-2(e1368)* mutants (Figure 1C) as well as *akt-1(ok525)* and *eak-7(tm3188)* single mutants, which develop reproductively at 25°C but arrest as dauers at 27°C (Figs. S1C-D) (Ailion and Thomas, 2003; Alam et al., 2010; Hu et al., 2006). In contrast, *set-4* mutation had no effect

on the dauer-constitutive phenotypes caused by mutations in *daf-1,* which encodes a Type 1 TGF-β receptor homolog (Georgi et al., 1990), or *daf-8,* which encodes a SMAD homolog (Park et al., 2010) (Figs. 1D and S1E). Similarly, *set-4* mutation did not suppress dauer arrest in animals harboring mutations in *daf-9* or *daf-36,* which encode DA biosynthesis pathway components (Figs. 1E and S1F) (Gerisch et al., 2001; Jia et al., 2002; Rottiers et al., 2006). Therefore, SET-4 acts specifically in the DAF-2/InsR pathway to promote dauer arrest.

Since previous reports link H4K20 methylation status to dosage compensation (Vielle et al., 2012; Wells et al., 2012), and DPY-21 promotes dauer arrest through dosage compensation (Dumas et al., 2013), we hypothesized that SET-4 may also regulate dauer arrest through dosage compensation. To test this, we determined the effect of *set-4* mutation on the dauer-constitutive phenotype of *eak-7;akt-1* double mutant hermaphrodites and males. If SET-4 promotes dauer arrest through the same mechanism as dosage compensation, then *set-4* mutation should suppress dauer in hermaphrodites but not males, since the DCC is inactive in males (Meyer, 2010). *dpy-21* and *set-4* mutations suppressed the dauer-constitutive phenotype of *eak-7;akt-1* hermaphrodites but did not affect dauer arrest in males (Figure 1F). Therefore, SET-4 may act through dosage compensation to control dauer arrest. We verified the role of SET-4 in dosage compensation by showing that *set-4* mutation suppressed lethality in *xol-1 sex-1* mutant males, which die due to inappropriate activation of dosage compensation (Dawes et al., 1999) (Figure S1G).

In order to determine whether SET-4 plays a role in regulating dauer entry in wild-type animals in response to physiologic stimuli, we tested the ability of dauer pheromone to induce dauer arrest in wild-type and *set-4* mutant animals. Mutation of either *set-4* or *dpy-21* decreased the sensitivity of wild-type animals to pheromone (Figure 1G). Therefore, SET-4 and DPY-21 promote dauer arrest in wild-type animals in response to increases in population density.

SET-4 is a H4K20 methyltransferase

The mammalian SET-4 ortholog SUV420H2 is a H4K20 methyltransferase (Schotta et al., 2004), and *C. elegans* SET-4 promotes H4K20 trimethylation (Vielle et al., 2012; Webster et al., 2013; Wells et al., 2012). We confirmed the requirement of SET-4 for H4K20 di- and trimethylation *in vivo* (Figure 2A). Immunoblots showed no detectable SET-4 protein in *set-4(n4600)* and *set-4(ok1481)* backgrounds, consistent with these being strong loss-of-function alleles. SET-4 protein levels in *set-4(dp268)* are comparable to wild-type (Figure

2A). H4K20me2 and H4K20me3 levels are undetectable in all three *set-4* mutant backgrounds (Figure 2A), suggesting that the S182F substitution in the SET domain abrogates catalytic activity. To test this possibility directly, we purified recombinant wild-type and mutant GST-SET-4 fusion proteins and tested their ability to methylate modified H4 peptides (H4K20me0, H4K20me1, and H4K20me2) *in vitro*. Mass spectrometry analysis revealed that both wild-type GST-SET-4 and GST-SUV420H2 were capable of converting H4K20me1 to H4K20me2 (Figure 2B-C). Consistent with *in vitro* experiments using human SET-4 orthologs SUV420H1 and SUV420H2 (Southall et al., 2014; Wu et al., 2013), methylation was not detected with unmethylated or dimethylated substrates, nor were trimethylated products detected in any assay (Figure 2B-C). It is possible that an enzyme distinct from SET-4 catalyzes H4K20 trimethylation *in vivo*. Alternatively, conversion of H4K20me2 to H4K20me3 by SET-4 *in vivo* may require a cofactor that is absent from our *in vitro* reactions.

GST-SET-4(S182F) did not methylate H4K20me1, indicating that the S182F mutation abolishes catalytic activity (Figure S2). Given that *set-4(dp268)* suppresses dauer to a similar extent as the two deletion alleles (Figure 1B), these data are consistent with SET-4 influencing dauer arrest through its conserved role in methylating H4K20.

SET-4 acts in neurons to promote dauer arrest

To determine where SET-4 is expressed, we generated strains expressing reporter genes under the control of *set-4* regulatory elements. Because two independent C-terminal SET-4::GFP translational fusions failed to rescue dauer arrest in *set-4* mutants, we generated strains expressing a *set-4p::*GFP promoter fusion to determine the spatiotemporal activity of the *set-4* promoter. *set-4p::*GFP transgenic animals expressed GFP broadly in embryos (Figure S3). Post-embryonically, we detected fluorescence predominantly in the head and tail regions of the animal, in a pattern consistent with neuronal expression. To confirm this, we established a transgenic strain that co-expressed *set-4p::*GFP and mCherry driven by the pan-neuronal *rab-3* promoter (Nonet et al., 1997). At all developmental stages interrogated, we observed co-localization of green and red fluorescence (Figure 3A), consistent with somatic *set-4p::*GFP expression being predominantly neuronal. We did not observe significant GFP expression in intestine, body wall muscle, or hypodermis.

As the amphid sensory neurons play a critical role in regulating dauer arrest (Bargmann and Horvitz, 1991; Schackwitz et al., 1996; Vowels and Thomas, 1994), we

interrogated them for expression of *set-4p::*GFP. Amphid neurons possess ciliary dendrites that are in direct contact with the environment and can be labeled with the lipophilic dye DiI (Starich et al., 1995). The extent of co-localization of green and red fluorescence in *set-4p::*GFP transgenic animals exposed to DiI (Figure 3B) reveals that the *set-4* promoter is active in amphid sensory neurons as well as in other cells.

To test whether neuronal expression of *set-4* is functionally important for dauer arrest, we generated tissue-specific *set-4* transgenes and tested them for the ability to rescue dauer arrest in *set-4* mutants. The neuronal *rab-3p::set-4* transgene rescued dauer formation to a similar extent as a *set-4* transgene driven by its native promoter (Figure 3C). In contrast, intestine-, hypodermis-, and muscle-specific *set-4* transgenes did not rescue dauer arrest to a greater extent than a transgene expressing the *set-4(dp268)* mutant. Taken together, these data indicate that SET-4 functions in the nervous system to promote dauer arrest.

Transcriptome-wide influences of DPY-21 and SET-4 on dauer regulation

We previously showed that the DCC component DPY-21 promotes DAF-16/FoxO activity (Dumas et al., 2013). To gain broader insight into how DPY-21 and SET-4 control dauer arrest, we performed whole transcriptome profiling to compare genome-wide regulatory influences (henceforth referred to as the "regulome") of DPY-21 and SET-4 to those of the key transcription factors controlling dauer arrest in *eak-7;akt-1* animals, DAF-16/FoxO and the nuclear receptor DAF-12 (Alam et al., 2010). We identified genes differentially expressed between wild-type and *eak-7;akt-1* double mutant animals [fold change ≥ 1.5 and false discovery rate (FDR) < 0.05]. We then compared the transcriptomes of *eak-7;akt-1* double mutants to those of *eak-7;akt-1* animals harboring mutations in *dpy-21, set-4*, *daf-16/FoxO,* or *daf-12,* and identified genes that are differentially expressed in the opposite direction as in wild-type relative to *eak-7;akt-1* (Table S1). Regulomes were validated by comparison with published data when possible (see below).

We defined the SET-4 dauer regulome by identifying 333 genes common to *set-4(n4600)* and *set-4(dp268)* regulomes (Table S1). Comparison of this gene set with SET-4-regulated genes identified in wild-type embryos and L3 larvae (Kramer et al., 2015) revealed minimal overlap [one gene (MTCE.34) among 94 regulated by SET-4 in embryos, and one gene (B0511.11) among 18 SET-4-regulated genes in L3 larvae]. This lack of concordance could be due to differences in genetic background (*eak-7;akt-1 vs.* wild-type), developmental stage (early L2 larvae *vs.* embryos/L3 larvae), and/or ambient temperature (25°C *vs.* 20°C).

A similar analysis with *eak-7;akt-1 dpy-21* mutants revealed 2,431 genes that comprise the DPY-21 dauer regulome (Table S1). To validate the DPY-21 regulome, we found significant overlap between the set of 700 X-linked genes differentially expressed in *eak-7;akt-1 dpy-21* vs. *eak-7;akt-1* animals with the 374 X-linked genes subject to dosage compensation in embryos (Jans et al., 2009) (119 genes; Figure S4A and Table S2; $p = 2.1e^{-26}$). 308 of 333 genes that comprise the SET-4 dauer regulome (92.5%) are also part of the DPY-21 dauer regulome (Figure 4A and Table S1), suggesting that a functional relationship between DPY-21 and SET-4 may exist in post-embryonic dauer regulation.

The DAF-16/FoxO regulome consists of 2,957 genes (Table S1). This gene set overlapped significantly with both the 469-gene young adult DAF-16/FoxO regulome (Chen et al., 2015) (203 common genes; Figure S4B and Table S3, $p = 3.2e^{-115}$) as well as the 1116-gene dauer regulome defined using *daf-7* TGFβ-like pathway mutants (Liu et al., 2004) (522 common genes; Figure S4C and Table S4, $p < 1e^{-100}$). Furthermore, 65 of the 132 genes regulated by the DAF-7 TGFβ-like pathway that contained at least one upstream DAF-16/FoxO binding motif (Liu et al., 2004) were part of the DAF-16/FoxO regulome [Figure S4D and Table S4 (bolded text), $p = 6.5e^{-42}$]. Most genes in the DAF-16/FoxO regulome (2,282 of 2,957 genes; 77.2%) are also regulated by DAF-12 (Figure 4B and Table S1). Over two-thirds of genes comprising both DAF-16/FoxO (2,041 of 2,957 genes; 69.0%; Table S1) and DAF-12 (1804 of 2556 genes; 70.6%; Table S1) regulomes are concordantly regulated by DPY-21.

The X-linked *ins-9* gene is repressed by DPY-21, SET-4 and DAF-16/FoxO

Based on genetic epistasis experiments (Dumas et al., 2013) (Figure 1), we hypothesized that DPY-21 and SET-4 influence DAF-16/FoxO activity through repression of X-linked genes. Moreover, in light of the neuronal site of action of SET-4 (Figure 3C) and its expression in amphid sensory neurons (Figure 3B), we speculated that key dauer regulatory genes subject to dosage compensation might function in a signaling capacity in the nervous system, upstream of DAF-12. Therefore, we examined the set of X-linked genes common to DPY-21 and DAF-16/FoxO regulomes that were *not* regulated by DAF-12, which acts downstream in the dauer regulatory cascade (Fielenbach and Antebi, 2008; Schaedel et al., 2012). This filtering strategy defined a set of 47 X-linked genes coordinately regulated by DPY-21 and DAF-16/FoxO but not influenced by *daf-12* mutation (Figure 4B; Table S5).

Among these X-linked genes was *ins-9,* which encodes one of 40 *C. elegans* ILPs (Pierce et al., 2001). Transcriptome profiling revealed that *ins-9* is silenced in *eak-7;akt-1* animals in a manner that requires both *daf-16/FoxO* and *dpy-21* (Table S2). We verified this by qPCR; *ins-9* expression was reduced more than 30-fold in *eak-7;akt-1* double mutants compared to wild-type animals (Figure 5A). Full repression required DAF-16/FoxO as well as DPY-21 and SET-4 but was independent of *daf-12*. Notably, a *daf-16/FoxO* null mutation did not restore *ins-9* transcript levels to wild-type levels. Furthermore, mutation of either *dpy-21* or *set-4* increased *ins-9* expression by substantially greater than two-fold (Figure 5A; 7.5-fold increase in *set-4;eak-7;akt-1* vs. *eak-7;akt-1*; 13.5-fold increase in *eak-7;akt-1 dpy-21* vs. *eak-7;akt-1*). Taken together, these observations suggest that DAF-16/FoxO and DPY-21/SET-4 act synergistically to repress *ins-9*.

ins-9 overexpression phenocopies dauer suppression caused by *dpy-21* or *set-4* mutation

INS-9 was an attractive candidate regulator of dauer arrest and DAF-2 ILS, as multiple ILPs have been shown to control dauer arrest through DAF-2/InsR (Cornils et al., 2011; Fernandes de Abreu et al., 2014; Hung et al., 2014; Li et al., 2003; Murphy et al., 2003; Pierce et al., 2001). If derepression of *ins-9* contributes to suppression of *eak-7;akt-1* dauer arrest in dosage compensation mutants, then *ins-9* overexpression should phenocopy dauer suppression caused by *set-4* or *dpy-21* mutation. We tested this by establishing transgenic

strains harboring a polycistronic construct which permitted expression of both *ins-9* and *mNeonGreen* (Shaner et al., 2013) fused to an SL2 leader sequence (Blumenthal, 2005) under the control of native *ins-9* 5' and 3' regulatory elements (*ins-9::SL2::mNG*). In two independent transgenic lines, *ins-9* overexpression (indicated by mNeonGreen detection) suppressed the dauer-constitutive phenotype of *eak-7;akt-1* double mutants (Figure 5B). Therefore, *ins-9* overexpression recapitulated the phenotype caused by *set-4* and *dpy-21* mutations (Dumas et al., 2013) (Figure 1B). These data are consistent with INS-9 acting as an agonist DAF-2/InsR ligand.

ins-9 is expressed specifically in a single pair of amphid neurons

Previous studies using reporters driven by the *ins-9* promoter suggested that *ins-9* is expressed in the ASI and ASJ amphid neurons as well as in additional tissues (Chen and Baugh, 2014; Pierce et al., 2001; Ritter et al., 2013). In contrast, in transgenic L2 larvae expressing *ins-9::SL2::mNG*, we consistently observed green fluorescence solely in one pair of sensory neurons. In animals in which neuronal morphology was discernable, we identified the fluorescent cells as the ASI amphid neurons (Figure 5C). We did not observe fluorescence in more than one pair of amphid neurons in any animal, nor did we detect fluorescence in other neurons or tissues. Since *ins-9::SL2::mNG* contains genomic elements from the *ins-9* locus that are missing from other reporters in the literature (Chen and Baugh, 2014; Pierce et al., 2001; Ritter et al., 2013), these observed patterns of expression are likely to be physiologically relevant.

ins-9 and *akt-2* are required for suppression of dauer arrest by *set-4* mutation

To determine the extent to which *ins-9* derepression contributes to dauer suppression in *set-4* mutants, we tested the ability of *set-4* to suppress the dauer-constitutive phenotype of *daf-2/InsR* mutants in wild-type and *ins-9* loss-of-function backgrounds. We generated strong loss-of-function *ins-9* alleles using CRISPR/Cas9 genome editing (Paix et al., 2015). Two probable null alleles, *dp675* and *dp677*, have nonsense mutations in the F-peptide region of *ins-9* that lies N-terminal to the functional B and A peptides (Pierce et al., 2001) (Figure S5). Although neither allele induced dauer arrest in a wild-type background, both *ins-9(dp675)* and *ins-9(dp677)* partially rescued dauer arrest in *set-4;daf-2* double mutants (Figure 5D),

indicating that dauer suppression caused by *set-4* mutation is due in part to de-repression of *ins-9*.

We previously showed that the X-linked gene *akt-2* is required for dauer suppression caused by *dpy-21* mutation (Dumas et al., 2013). We verified that *akt-2* transcripts increase two-fold in *eak-7;akt-1* double mutants when *set-4* or *dpy-21* is mutated (Figure S6A). Similar to *ins-9* mutation, *akt-2* mutation also partially rescued dauer arrest in animals lacking *set-4* (Figure 5E), and the phenotypic effects of *ins-9* and *akt-2* mutations on dauer arrest may be additive (Figure 5E). However, *set-4;daf-2;ins-9 akt-2* compound mutant animals still did not undergo dauer arrest to the same extent as *daf-2* single mutant animals (Figure 5E), indicating that regulation of additional genes may contribute to dauer arrest.

The autosomal *ins-7* gene contributes to suppression of dauer arrest by *set-4* mutation

As the only X-linked *ins* gene, *ins-9* is the sole *ins* gene subject to direct regulation by dosage compensation or other X-chromosome-specific mechanisms of gene regulation. However, it is conceivable that other *ins* genes could contribute to dauer regulation through indirect effects on their expression. Genes encoding three agonist ILPs, INS-4, INS-6, and DAF-28, are expressed in the ASI sensory neurons and have established roles in inhibiting dauer arrest and promoting reproductive development (Cornils et al., 2011; Hung et al., 2014; Li et al., 2003). To determine whether regulation of *ins-4, ins-6,* and/or *daf-28* contributes to dauer suppression in this context, we measured *ins-4, ins-6,* and *daf-28* transcript levels in wild-type, *eak-7;akt-1* double mutant, and *eak-7;akt-1* triple mutants with reduced DPY-21 or SET-4 activity. None of these genes was repressed in *eak-7;akt-1* double mutants compared to wild-type animals, nor did loss of *set-4* or *dpy-21* cause significant increases in their expression (Figure S6B-D). Therefore, neither DPY-21 nor SET-4 influences dauer arrest through regulation of *ins-4, ins-6,* and *daf-28* expression.

To determine whether other ILPs could contribute to dauer regulation by DPY-21 or SET-4, we searched the set of genes common to DAF-16/FoxO and DPY-21 regulomes for *ins* genes. Seven *ins* genes are concordantly regulated by DAF-16/FoxO and DPY-21 based on FPKM counts from whole transcriptome data (Table S6). Two genes encoding putative antagonist ILPs, *ins-20* and *ins-11* (Fernandes de Abreu et al., 2014), are repressed by DAF-16/FoxO and DPY-21; however, an increase in their expression in *dpy-21* mutants would be expected to enhance, rather than suppress, dauer arrest. Similarly, two *ins* genes encoding agonist ILPs, *ins-33* and *ins-35* (Fernandes de Abreu et al., 2014; Michaelson et al., 2010),

are induced by DAF-16/FoxO and DPY-21; a decrease in their expression in *dpy-21* mutants would also be expected to enhance dauer arrest if changes in their expression were functionally important in dauer regulation. DAF-16/FoxO and DPY-21 induce the expression of two *ins* genes of unknown function, *ins-16* and *ins-29* (Fernandes de Abreu et al., 2014). Finally, *ins-7,* which encodes an agonist ILP (Murphy et al., 2007; Murphy et al., 2003), is repressed by DAF-16/FoxO and DPY-21 (Murphy et al., 2007; Murphy et al., 2003) (Table S6). As *ins-7* and *ins-9* both encode agonist ILPs, are concordantly regulated by DAF-16/FoxO and DPY-21, and have been shown to influence dauer arrest (Murphy et al., 2007; Murphy et al., 2003) (Figure 5C-E), we tested *ins-7* for a role in promoting reproductive development in *dpy-21* and *set-4* mutants. We verified *ins-7* repression by DAF-16/FoxO, SET-4, and DPY-21 using qPCR (Figure S6E). The *ins-7(tm1907)* deletion allele partially rescued dauer in *set-4;daf-2* animals and may have an additive effect with *ins-9* mutation on dauer suppression (Figure 5F). Thus, SET-4 may influence dauer arrest through both direct repression of X-linked genes such as *ins-9* and *akt-2* and perhaps indirect regulation of autosomal dauer regulatory genes such as *ins-7*.

DISCUSSION

Although much is known about the conserved signaling pathways that control *C. elegans* dauer arrest, how these pathways are regulated by upstream inputs is poorly understood. In the present study, we have established a framework for understanding how DPY-21 and SET-4 promote dauer arrest in the context of reduced DAF-2 ILS. Specifically, we have discovered that the conserved H4K20 methyltransferase SET-4 acts in the nervous system to promote dauer arrest. It does so in part by synergizing with DAF-16/FoxO to repress the X-linked insulin-like peptide gene *ins-9*. We hypothesize that SET-4 and DPY-21 act similarly to directly repress *ins-9* and *akt-2,* thus attenuating DAF-2 ILS and promoting dauer arrest through activation of DAF-16/FoxO (Figure 6).

Although INS-9 has been predicted to function as an agonist ILP based on both structural models indicating similarity to the agonist ILPs INS-4, INS-6, and DAF-28 (Pierce et al., 2001) and expression changes upon starvation and feeding of larvae (Chen and Baugh, 2014), analysis of existing *ins-9* mutants has not revealed phenotypes consistent with this (Fernandes de Abreu et al., 2014). This may be due to *ins-9(tm3618)* not being a strong loss-of-function allele. In contrast, our analysis of transgenic animals overexpressing *ins-9* (Figure 5B) and mutant animals harboring nonsense *ins-9* alleles (Figure 5D-F) provides the first experimental evidence demonstrating that INS-9 is an agonist ILP.

Several ILPs have been implicated in dauer regulation (Cornils et al., 2011; Fernandes de Abreu et al., 2014; Hung et al., 2014; Li et al., 2003; Murphy et al., 2003; Pierce et al., 2001). However, the mechanistic basis for how environmental cues regulate ILPs remains obscure. The initial events that control dauer arrest through DAF-2 ILS likely take place in the amphid sensory neurons, which are required for dauer formation in response to pheromone (Schackwitz et al., 1996; Vowels and Thomas, 1994). Indeed, genes encoding INS-4, INS-6, and DAF-28, which collectively play a major role in promoting reproductive development through DAF-2 ILS (Cornils et al., 2011; Hung et al., 2014; Li et al., 2003), are expressed in ASI (Chen and Baugh, 2014; Cornils et al., 2011; Hung et al., 2014; Li et al., 2003), and the transcription of *ins-6* and *daf-28* is inhibited by dauer pheromone through unknown mechanisms (Cornils et al., 2011; Li et al., 2003). Our finding that DPY-21 and SET-4 influence dauer arrest in part by repressing the X-linked *ins-9* gene provides a potential mechanistic link between a dauer-regulatory environmental cue and an ILP expressed in sensory neurons that control the dauer decision.

An intriguing but incompletely understood aspect of dauer morphogenesis is the mechanistic basis for the commitment of larvae to either the reproductive or dauer developmental fate. Assays in which larvae are shifted between favorable and unfavorable conditions at different times after hatching indicate the existence of commitment points beyond which animals develop reproductively or arrest as dauers regardless of ambient conditions (Golden and Riddle, 1984; Schaedel et al., 2012). Commitment to reproductive development correlates temporally with the activation of a feed-forward loop amplifying organismal DA biosynthesis through DA-dependent induction of DAF-9 expression in the hypodermis (Schaedel et al., 2012). However, the XXX cells (Ohkura et al., 2003), thought to be the sole source of DA biosynthesis prior to the commitment point (Schaedel et al., 2012), are not in direct contact with the environment. Therefore, they must receive upstream inputs from sensory neurons that convey information about ambient conditions.

Our finding that DPY-21 and SET-4 synergize with DAF-16/FoxO to repress *ins-9* is consistent with a hypothetical model in which INS-9 may function as a key node in an autocrine feed-forward loop in the ASI sensory neurons that reinforces levels of its own expression in response to changing environments, upstream of DA biosynthesis in the XXX cells and hypodermis. In replete conditions, *ins-9* expression in ASI is expected to lead to activation of DAF-2 ILS and inhibition of DAF-16/FoxO. Since DAF-16/FoxO inhibits *ins-9* expression, decreased DAF-16/FoxO activity would lead to increased *ins-9* expression, which would presumably lead to further activation of DAF-2 ILS and inhibition of DAF-16/FoxO, both in an autocrine fashion in ASI as well as in other cells that express DAF-2/InsR. In the context of increased population density, pheromone would promote *ins-9* repression through DPY-21 and SET-4 and reduce autocrine and paracrine engagement of DAF-2/InsR, resulting in DAF-16/FoxO activation, further repression of *ins-9,* and dauer arrest (Figure 6). The effect of DPY-21 and SET-4 would not be limited to sensory neurons, as they would also act in other cells responding to INS-9 to control their sensitivity to ILPs by repressing *akt-2* (Dumas et al., 2013) (Figures 6 and S6A). In addition, *ins-9* regulation may also be amplified through other ILPs such as INS-7, which functions in a feed-forward loop in adults to coordinate DAF-16/FoxO activity throughout the animal (Murphy et al., 2007).

MATERIALS AND METHODS

C. elegans strains and maintenance

Mutant alleles are listed in Supplementary Materials and Methods. Compound mutants were generated using standard protocols. All animals were maintained on nematode growth media (NGM) plates seeded with *E. coli* OP50 using standard techniques.

Dauer arrest assays

Dauer arrest assays were performed as previously described (Hu et al., 2006). *daf-9(dh6)* mutant animals were propagated on NGM plates supplemented with 10 nM Δ^7-DA, then transferred to NGM plates for egglays as previously described (Dumas et al., 2013). For male dauer assays, males were crossed to isogenic L4 hermaphrodites, and the gender of dauer progeny was determined after dauer exit.

Dauer pheromone assays

Dauer pheromone was prepared as previously described (Golden and Riddle, 1982; Schroeder and Flatt, 2014). Details are provided in Supplementary Materials and Methods.

Generation of transgenic strains

Details pertaining to the generation of reporter constructs and transgenic strains are provided in Supplementary Materials and Methods.

CRISPR/Cas9-based mutagenesis

ins-9(dp675) and *ins-9(dp677)* were generated using recombinant crRNA and tracrRNA (Dharmacon) and Cas9 (PNA Bio) as described (Paix et al., 2015). See Table S7 for sequences of guide RNAs and repair oligonucleotides.

RNA isolation

Greater than 200 gravid hermaphrodites were allowed to lay eggs for 6 hr at 20°C and then removed. Eggs were transferred to 25°C for 24 hr. Larvae were harvested, washed once in M9 buffer and once in water, and resuspended in TRIzol (Invitrogen). After five sequential freeze-thaws, RNA was extracted using chloroform. Extracted RNA was purified using a Direct-zol RNA Miniprep Kit (Zymo Research).

qPCR

cDNA was synthesized with oligo-dT priming using the SuperScript III First Strand Synthesis Kit (Invitrogen). The equivalent of 10 ng of starting RNA was used as template in a 15 μL reaction using the Quantitect SYBRgreen qPCR Kit (Qiagen). Reactions were performed in a RotorGene 6000 (Corbett Research) and results analyzed using RotorGene 6000 Software (version 1.7). Samples were normalized to *pmp-3* expression prior to comparison between groups (Hoogewijs et al., 2008). See Table S8 for primer sequences. Relative expression was calculated as described (Nolan et al., 2006).

Confocal microscopy

Animals were mounted on slides layered with a thin 3% agarose pad containing 25 mM sodium azide. Images were captured on a Leica Inverted SP5X Confocal Microscope (Leica) using LAS AF software.

RNA-seq analysis

Whole transcriptome profiling was performed by the University of Michigan DNA Sequencing Core as previously described (Chen et al., 2015) using 100 ng input RNA per sample. Samples were barcoded and multiplexed, and 100-nucleotide paired end sequencing was performed using an Illumina HiSeq 2000 sequencer and Version 4 reagents. Five experimental replicates were analyzed. Correlation coefficients between replicates and genotypes are shown in Table S9.

Annotated gene expression data output from CuffDiff v2.2.1 (Trapnell et al., 2013) was read into R version 3.2.1(2015-06-18; The R Foundation for Statistical Computing; http://www.r-project.org/) for six comparisons: *eak-7;akt-1* compared to (1) wild-type, (2) *daf-16(mu86);eak-7;akt-1*, (3) *daf-12;eak-7;akt-1*, (4) set-*4(n4600);eak-7;akt-1*, (5) *set-4(dp268);eak-7;akt-1*, and (6) *dpy-21;eak-7;akt-1*. We filtered genes by the following criteria: (1) status = "OK" for wild-type *vs. eak-7;akt-1,* (2) fold change (FC) ≥ 1.5 or FC ≤ 1/1.5 for wild-type *vs. eak-7;akt-1* and (3) FDR < 0.05 for at least two separate comparisons.

DAF-16 targets were defined as those filtered genes that also met (1) status = "OK" for *eak-7;akt-1 vs. daf-16;eak-7;akt-1*, and (2) FC ≥ 1.5 for *eak-7;akt-1 vs. daf-16;eak-7;akt-1* in the opposite direction as wild-type *vs. eak-7;akt-1*. DPY-21, SET-4, and DAF-12 targets were determined in an analogous fashion. For SET-4, we generated a list of SET-4 targets that showed FC ≥ 1.5 or FC ≤ 1/1.5 for both *set-4* alleles, and a list that showed these changes for either one or both *set-4* alleles. Lists of overlapping targets were then generated from these target lists.

Significance of overlap with dosage-compensated X-linked genes (Jans et al., 2009), strongly regulated dauer genes (Liu et al., 2004), and DAF-16 targets in the *daf-2(e1370)* background (Chen et al., 2015) was calculated using a hypergeometric distribution, assuming 5863 X-linked transcripts and 46233 genome-wide transcripts in *C. elegans* detected in our RNA-seq analysis (by either the UCSCce10 reference transcriptome or *de novo* transcript assembly). If necessary, common WormBase Gene identifiers were downloaded from WormBase version WS250 (intermine.wormbase.org).

Immunoblotting and antibodies

To generate protein lysates, animals were washed in M9, then in sterile water. Pelleted animals were resuspended in equal volumes of worm lysis buffer (Webster et al., 2013), incubated at 85°C for 5 min, then sonicated on ice for two cycles of 30 seconds each at 70% power using a Sonic Dismembrator Model 100 (Fisher Scientific). Homogenates were quantified using a DC^{TM} Protein Quantification Kit (BioRad). 50 μg protein was loaded per lane using Criterion systems (BioRad) and transferred to Immobilon Psq (Millipore). Details pertaining to antibodies are provided in Supplementary Materials and Methods. Membranes were blocked with 5% milk in TBS + 0.5% Tween 20. Antibodies were diluted in Western Blocking Solution (Sigma) prior to incubation with membranes. Blots were washed with TBS + 0.5% Tween 20. Signal was detected by ECL (Pierce).

Histone methyltransferase assay

set-4 cDNAs were amplified from RNA isolated from wild-type or *set-4(dp268)* mutant animals. Human *Suv420H2* cDNA was obtained from Origene. Clones were ligated into pGEX4T1 vector (GE Healthcare). Protein expression was induced overnight at 16°C with 0.1 mM IPTG in BL21-CodonPlus(DE3)-RIPL cells (Agilent Technologies) grown in Terrific Broth (Invitrogen) + 4% glycerol (Sigma). Cells were disrupted using a Sonic Dismembrator Model 100 sonicator (Fisher Scientific), with four cycles of ten one-second on/off pulses of 10-30% intensity. Lysates were cleared by centrifugation at 20,000g for 5 min and incubated with Glutathione-Sepharose beads (GE Healthcare) rotating overnight at 4°C. Expression of recombinant protein was confirmed by Coomassie staining and anti-GST immunoblot. Beads bound to recombinant protein were incubated in 10 mM Tris pH 8.0, 2 μM β-mercaptoethanol, and 7 mM S-adenosylmethionine (Sigma) in the presence of 2 mM substrate peptide corresponding to amino acids 8-30 of *C. elegans* histone H4 (AnaSpec) rotating for 4 hr at 30°C. Reactions were analyzed using a Waters MicroMass MALDI-TOF mass spectrometer and analyzed with MassLynx software. Ratios of peak heights corresponding to reactant and product peptide were calculated to define percent conversion.

Male rescue assay

Mated gravid hermaphrodites were placed on NGM plates to lay eggs for 24 hr at 20°C. Egglayers were removed, and the number of hatchlings and eggs were counted. After 72 hr, the animals were moved to 4°C to slow movement. Male rescue was calculated as the ratio of live males to total eggs laid. Each experiment was performed in triplicate.

Statistics

Two-tailed Student's t-test was used to measure significance in experiments unless otherwise noted. Data is presented as the average and standard error of the means of at least three biological replicates, each replicate performed in triplicate. N's for dauer assays are listed from left to right.

Data availability

Strains are available upon request. Whole transcriptome profiling data are available at GEO with the accession number: GSE89295.

ACKNOWLEDGEMENTS

REFERENCES

Ailion, M. and Thomas, J. H. (2003). Isolation and characterization of high-temperature-induced Dauer formation mutants in Caenorhabditis elegans. *Genetics* **165**, 127-144.

Alam, H., Williams, T. W., Dumas, K. J., Guo, C., Yoshina, S., Mitani, S. and Hu, P. J. (2010). EAK-7 controls development and life span by regulating nuclear DAF-16/FoxO activity. *Cell Metab* **12**, 30-41.

Andersen, E. C. and Horvitz, H. R. (2007). Two C. elegans histone methyltransferases repress lin-3 EGF transcription to inhibit vulval development. *Development* **134**, 2991-2999.

Bargmann, C. I. and Horvitz, H. R. (1991). Control of larval development by chemosensory neurons in Caenorhabditis elegans. *Science* **251**, 1243-1246.

Blumenthal, T. (2005). Trans-splicing and operons. *WormBook*, 1-9.

Butcher, R. A., Ragains, J. R., Kim, E. and Clardy, J. (2008). A potent dauer pheromone component in Caenorhabditis elegans that acts synergistically with other components. *Proc Natl Acad Sci U S A* **105**, 14288-14292.

Chen, A. T., Guo, C., Itani, O. A., Budaitis, B. G., Williams, T. W., Hopkins, C. E., McEachin, R. C., Pande, M., Grant, A. R., Yoshina, S., et al. (2015). Longevity Genes Revealed by Integrative Analysis of Isoform-Specific daf-16/FoxO Mutants of Caenorhabditis elegans. *Genetics* **201**, 613-629.

Chen, Y. and Baugh, L. R. (2014). Ins-4 and daf-28 function redundantly to regulate C. elegans L1 arrest. *Dev Biol* **394**, 314-326.

Cornils, A., Gloeck, M., Chen, Z., Zhang, Y. and Alcedo, J. (2011). Specific insulin-like peptides encode sensory information to regulate distinct developmental processes. *Development* **138**, 1183-1193.

Dawes, H. E., Berlin, D. S., Lapidus, D. M., Nusbaum, C., Davis, T. L. and Meyer, B. J. (1999). Dosage compensation proteins targeted to X chromosomes by a determinant of hermaphrodite fate. *Science* **284**, 1800-1804.

Dumas, K. J., Delaney, C. E., Flibotte, S., Moerman, D. G., Csankovszki, G. and Hu, P. J. (2013). Unexpected Role for Dosage Compensation in the Control of Dauer Arrest, Insulin-Like Signaling, and FoxO Transcription Factor Activity in Caenorhabditis elegans. *Genetics* **194**, 619-629.

Fernandes de Abreu, D. A., Caballero, A., Fardel, P., Stroustrup, N., Chen, Z., Lee, K., Keyes, W. D., Nash, Z. M., Lopez-Moyado, I. F., Vaggi, F., et al. (2014). An insulin-to-insulin regulatory network orchestrates phenotypic specificity in development and physiology. *PLoS Genet* **10**, e1004225.

Fielenbach, N. and Antebi, A. (2008). C. elegans dauer formation and the molecular basis of plasticity. *Genes Dev* **22**, 2149-2165.

Georgi, L. L., Albert, P. S. and Riddle, D. L. (1990). daf-1, a C. elegans gene controlling dauer larva development, encodes a novel receptor protein kinase. *Cell* **61**, 635-645.

Gerisch, B., Weitzel, C., Kober-Eisermann, C., Rottiers, V. and Antebi, A. (2001). A hormonal signaling pathway influencing C. elegans metabolism, reproductive development, and life span. *Developmental cell* **1**, 841-851.

Golden, J. W. and Riddle, D. L. (1982). A pheromone influences larval development in the nematode Caenorhabditis elegans. *Science* **218**, 578-580.

---- (1984). The Caenorhabditis elegans dauer larva: developmental effects of pheromone, food, and temperature. *Dev Biol* **102**, 368-378.

Gottlieb, S. and Ruvkun, G. (1994). daf-2, daf-16 and daf-23: genetically interacting genes controlling Dauer formation in Caenorhabditis elegans. *Genetics* **137**, 107-120.

Hoogewijs, D., Houthoofd, K., Matthijssens, F., Vandesompele, J. and Vanfleteren, J. R. (2008). Selection and validation of a set of reliable reference genes for quantitative sod gene expression analysis in C. elegans. *BMC Mol Biol* **9**, 9.

Hu, P. J., Xu, J. and Ruvkun, G. (2006). Two membrane-associated tyrosine phosphatase homologs potentiate C. elegans AKT-1/PKB signaling. *PLoS Genet* **2**, e99.

Hung, W. L., Wang, Y., Chitturi, J. and Zhen, M. (2014). A Caenorhabditis elegans developmental decision requires insulin signaling-mediated neuron-intestine communication. *Development* **141**, 1767-1779.

Jans, J., Gladden, J. M., Ralston, E. J., Pickle, C. S., Michel, A. H., Pferdehirt, R. R., Eisen, M. B. and Meyer, B. J. (2009). A condensin-like dosage compensation complex acts at a distance to control expression throughout the genome. *Genes Dev* **23**, 602-618.

Jia, K., Albert, P. S. and Riddle, D. L. (2002). DAF-9, a cytochrome P450 regulating C. elegans larval development and adult longevity. *Development* **129**, 221-231.

Kramer, M., Kranz, A. L., Su, A., Winterkorn, L. H., Albritton, S. E. and Ercan, S. (2015). Developmental Dynamics of X-Chromosome Dosage Compensation by the DCC and H4K20me1 in C. elegans. *PLoS Genet* **11**, e1005698.

Li, W., Kennedy, S. G. and Ruvkun, G. (2003). daf-28 encodes a C. elegans insulin superfamily member that is regulated by environmental cues and acts in the DAF-2 signaling pathway. *Genes Dev* **17**, 844-858.

Liu, T., Zimmerman, K. K. and Patterson, G. I. (2004). Regulation of signaling genes by TGFbeta during entry into dauer diapause in C. elegans. *BMC developmental biology* **4**, 11.

Meyer, B. J. (2010). Targeting X chromosomes for repression. *Curr Opin Genet Dev* **20**, 179-189.

Michaelson, D., Korta, D. Z., Capua, Y. and Hubbard, E. J. (2010). Insulin signaling promotes germline proliferation in C. elegans. *Development* **137**, 671-680.

Murphy, C. T. and Hu, P. J. (2013). Insulin/insulin-like growth factor signaling in C. elegans. *WormBook*, 1-43.

Murphy, C. T., Lee, S. J. and Kenyon, C. (2007). Tissue entrainment by feedback regulation of insulin gene expression in the endoderm of Caenorhabditis elegans. *Proc Natl Acad Sci U S A* **104**, 19046-19050.

Murphy, C. T., McCarroll, S. A., Bargmann, C. I., Fraser, A., Kamath, R. S., Ahringer, J., Li, H. and Kenyon, C. (2003). Genes that act downstream of DAF-16 to influence the lifespan of Caenorhabditis elegans. *Nature* **424**, 277-283.

Nolan, T., Hands, R. E. and Bustin, S. A. (2006). Quantification of mRNA using real-time RT-PCR. *Nat Protoc* **1**, 1559-1582.

Nonet, M. L., Staunton, J. E., Kilgard, M. P., Fergestad, T., Hartwieg, E., Horvitz, H. R., Jorgensen, E. M. and Meyer, B. J. (1997). Caenorhabditis elegans rab-3 mutant synapses exhibit impaired function and are partially depleted of vesicles. *The Journal of neuroscience : the official journal of the Society for Neuroscience* **17**, 8061-8073.

Ohkura, K., Suzuki, N., Ishihara, T. and Katsura, I. (2003). SDF-9, a protein tyrosine phosphatase-like molecule, regulates the L3/dauer developmental decision through hormonal signaling in C. elegans. *Development* **130**, 3237-3248.

Paix, A., Folkmann, A., Rasoloson, D. and Seydoux, G. (2015). High Efficiency, Homology-Directed Genome Editing in Caenorhabditis elegans Using CRISPR-Cas9 Ribonucleoprotein Complexes. *Genetics* **201**, 47-54.

Park, D., Estevez, A. and Riddle, D. L. (2010). Antagonistic Smad transcription factors control the dauer/non-dauer switch in C. elegans. *Development* **137**, 477-485.

Pierce, S. B., Costa, M., Wisotzkey, R., Devadhar, S., Homburger, S. A., Buchman, A. R., Ferguson, K. C., Heller, J., Platt, D. M., Pasquinelli, A. A., et al. (2001). Regulation of DAF-2 receptor signaling by human insulin and ins-1, a member of the unusually large and diverse C. elegans insulin gene family. *Genes Dev* **15**, 672-686.

Ren, P., Lim, C. S., Johnsen, R., Albert, P. S., Pilgrim, D. and Riddle, D. L. (1996). Control of C. elegans larval development by neuronal expression of a TGF-beta homolog. *Science* **274**, 1389-1391.

Riddle, D. L. (1988). The Dauer Larva. In *The Nematode Caenorhabditis elegans* (ed. W. B. Wood, editor), pp. 393-412. Plainview (New York): Cold Spring Harbor Laboratory Press.

Riddle, D. L., Swanson, M. M. and Albert, P. S. (1981). Interacting genes in nematode dauer larva formation. *Nature* **290**, 668-671.

Ritter, A. D., Shen, Y., Fuxman Bass, J., Jeyaraj, S., Deplancke, B., Mukhopadhyay, A., Xu, J., Driscoll, M., Tissenbaum, H. A. and Walhout, A. J. (2013). Complex expression dynamics and robustness in C. elegans insulin networks. *Genome Res* **23**, 954-965.

Rottiers, V., Motola, D. L., Gerisch, B., Cummins, C. L., Nishiwaki, K., Mangelsdorf, D. J. and Antebi, A. (2006). Hormonal control of C. elegans dauer formation and life span by a Rieske-like oxygenase. *Developmental cell* **10**, 473-482.

Schackwitz, W. S., Inoue, T. and Thomas, J. H. (1996). Chemosensory neurons function in parallel to mediate a pheromone response in C. elegans. *Neuron* **17**, 719-728.

Schaedel, O. N., Gerisch, B., Antebi, A. and Sternberg, P. W. (2012). Hormonal signal amplification mediates environmental conditions during development and controls an irreversible commitment to adulthood. *PLoS Biol* **10**, e1001306.

Schotta, G., Lachner, M., Sarma, K., Ebert, A., Sengupta, R., Reuter, G., Reinberg, D. and Jenuwein, T. (2004). A silencing pathway to induce H3-K9 and H4-K20 trimethylation at constitutive heterochromatin. *Genes Dev* **18**, 1251-1262.

Schroeder, N. E. and Flatt, K. M. (2014). In vivo imaging of Dauer-specific neuronal remodeling in C. elegans. *Journal of visualized experiments : JoVE*, e51834.

Shaner, N. C., Lambert, G. G., Chammas, A., Ni, Y., Cranfill, P. J., Baird, M. A., Sell, B. R., Allen, J. R., Day, R. N., Israelsson, M., et al. (2013). A bright monomeric green fluorescent protein derived from Branchiostoma lanceolatum. *Nat Methods* **10**, 407-409.

Southall, S. M., Cronin, N. B. and Wilson, J. R. (2014). A novel route to product specificity in the Suv4-20 family of histone H4K20 methyltransferases. *Nucleic Acids Res* **42**, 661-671.

Starich, T. A., Herman, R. K., Kari, C. K., Yeh, W. H., Schackwitz, W. S., Schuyler, M. W., Collet, J., Thomas, J. H. and Riddle, D. L. (1995). Mutations affecting the chemosensory neurons of Caenorhabditis elegans. *Genetics* **139**, 171-188.

Thomas, J. H., Birnby, D. A. and Vowels, J. J. (1993). Evidence for parallel processing of sensory information controlling dauer formation in Caenorhabditis elegans. *Genetics* **134**, 1105-1117.

Trapnell, C., Hendrickson, D. G., Sauvageau, M., Goff, L., Rinn, J. L. and Pachter, L. (2013). Differential analysis of gene regulation at transcript resolution with RNA-seq. *Nat Biotechnol* **31**, 46-53.

Vielle, A., Lang, J., Dong, Y., Ercan, S., Kotwaliwale, C., Rechtsteiner, A., Appert, A., Chen, Q. B., Dose, A., Egelhofer, T., et al. (2012). H4K20me1 contributes to downregulation of X-linked genes for C. elegans dosage compensation. *PLoS Genet* **8**, e1002933.

Vowels, J. J. and Thomas, J. H. (1992). Genetic analysis of chemosensory control of dauer formation in Caenorhabditis elegans. *Genetics* **130**, 105-123.

---- (1994). Multiple chemosensory defects in daf-11 and daf-21 mutants of Caenorhabditis elegans. *Genetics* **138**, 303-316.

Webster, C. M., Wu, L., Douglas, D. and Soukas, A. A. (2013). A non-canonical role for the C. elegans dosage compensation complex in growth and metabolic regulation downstream of TOR complex 2. *Development* **140**, 3601-3612.

Wells, M. B., Snyder, M. J., Custer, L. M. and Csankovszki, G. (2012). Caenorhabditis elegans dosage compensation regulates histone H4 chromatin state on X chromosomes. *Mol Cell Biol* **32**, 1710-1719.

Wu, H., Siarheyeva, A., Zeng, H., Lam, R., Dong, A., Wu, X. H., Li, Y., Schapira, M., Vedadi, M. and Min, J. (2013). Crystal structures of the human histone H4K20 methyltransferases SUV420H1 and SUV420H2. *FEBS Lett* **587**, 3859-3868.

Yonker, S. A. and Meyer, B. J. (2003). Recruitment of C. elegans dosage compensation proteins for gene-specific versus chromosome-wide repression. *Development* **130**, 6519-6532.

Figures
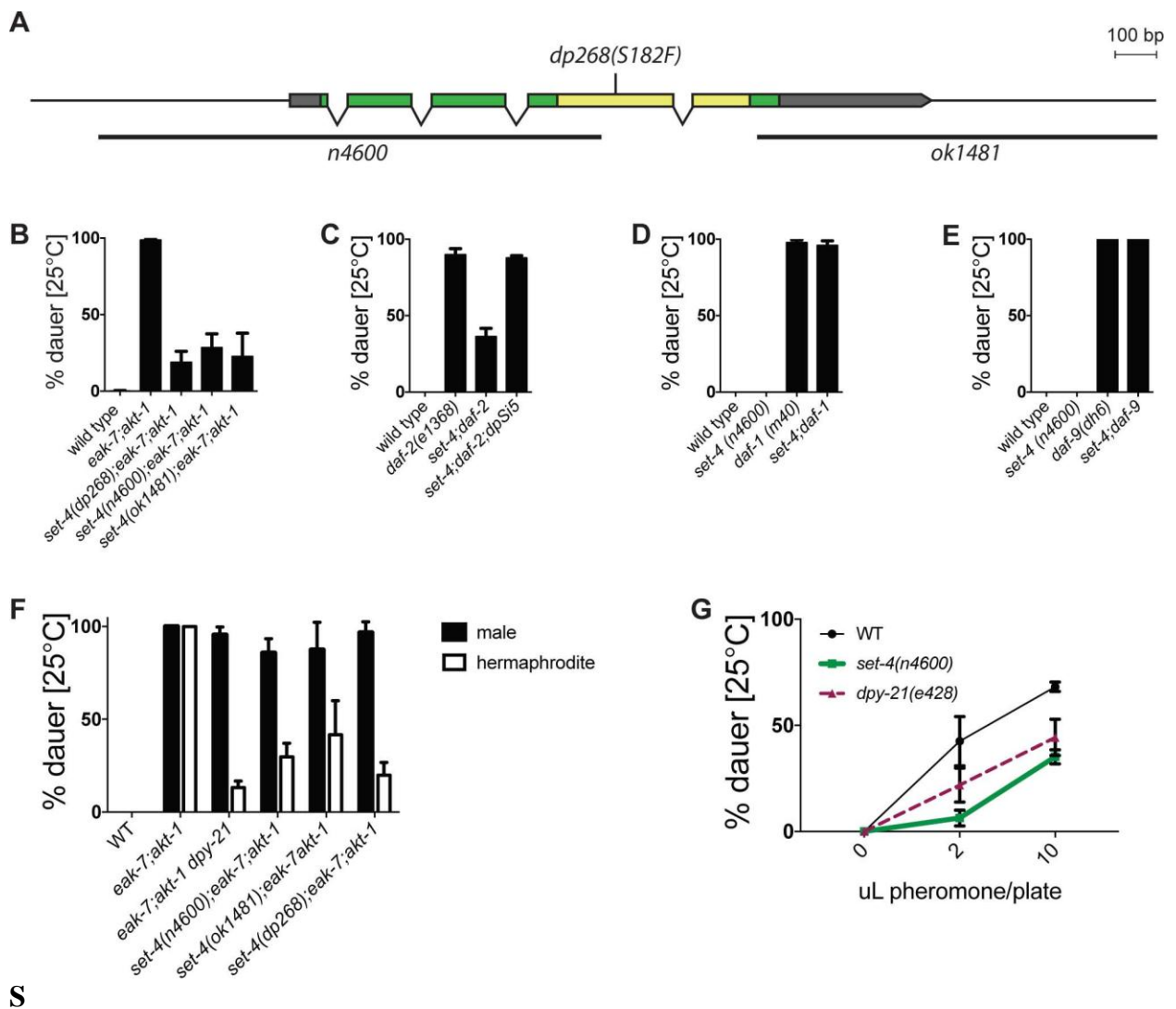
Figure 1. SET-4 promotes dauer arrest. (**A**) Schematic of the *set-4* locus and three mutant alleles. Exons are indicated as boxes, separated by introns. Gray, green, and yellow denote untranslated regions, coding sequence, and SET domain coding sequence, respectively. Deletions are indicated by black bars. (**B**) *set-4* mutations suppress the dauer-constitutive phenotype of *eak-7;akt-1* mutants [N (left to right) = 236, 627, 389, 521, 638]. (**C**) *set-4(n4600)* suppresses the dauer-constitutive phenotype of *daf-2(e1368)* mutants and is rescued by the single-copy *set-4* transgene *dpSi5* (N = 913, 1668, 1568, 1785). *set-4* is dispensable for dauer arrest in (**D**) *daf-1(m40)* (N = 2215, 2189, 1816, 1899) and (**E**) *daf-9(dh6)* mutants (N = 1753, 1561, 2188, 2486). (**F**) *set-4* and *dpy-21* mutations suppress dauer arrest in XX hermaphrodites but not XO males (N = 567, 1330, 579, 1003, 1012, 700). (**G**) *set-4* and *dpy-21* mutations attenuate the response of wild-type animals to dauer pheromone [N (0uL, 2uL,

10uL): wild type = 542, 461, 544; *set-4* = 413, 246, 387; *dpy-21* = 334, 220, 275.]. *set-4* vs. wild type: p < 0.01 by two-way ANOVA.
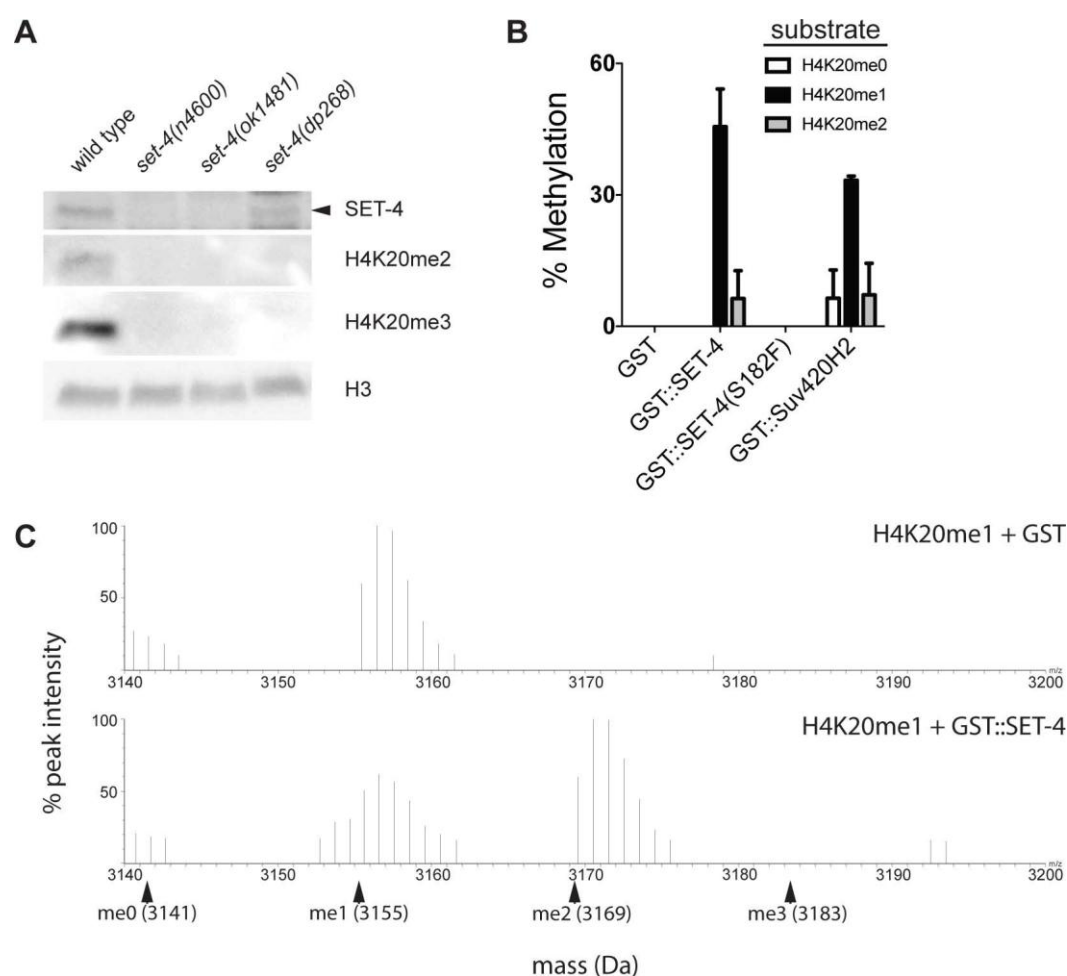
Figure 2. SET-4 is a histone H4K20 methyltransferase. (**A**) SET-4 promotes H4K20 methylation *in vivo.* Anti-SET-4, H4K20me2, H4K20me3, and H3 immunoblots of lysates from wild-type and *set-4* mutant animals are shown. SET-4 protein is indicated by the arrowhead. Images are representative of four biological replicates. (**B**) Recombinant GST-SET-4 fusion protein methylates H4K20me1 *in vitro.* Percent methylation of H4K20 peptide substrates by GST proteins fused to wild-type SET-4, mutant SET-4(S182F), or human SET-4 ortholog SUV420H2 is shown. Data represent mean values from three biological replicates. (**C**) MALDI spectra illustrating conversion of H4K20me1 to H4K20me2 by GST-SET-4. Monoisotopic masses (protonated) of peptide substrates are indicated with arrowheads. Spectra are representative of three independent experiments.
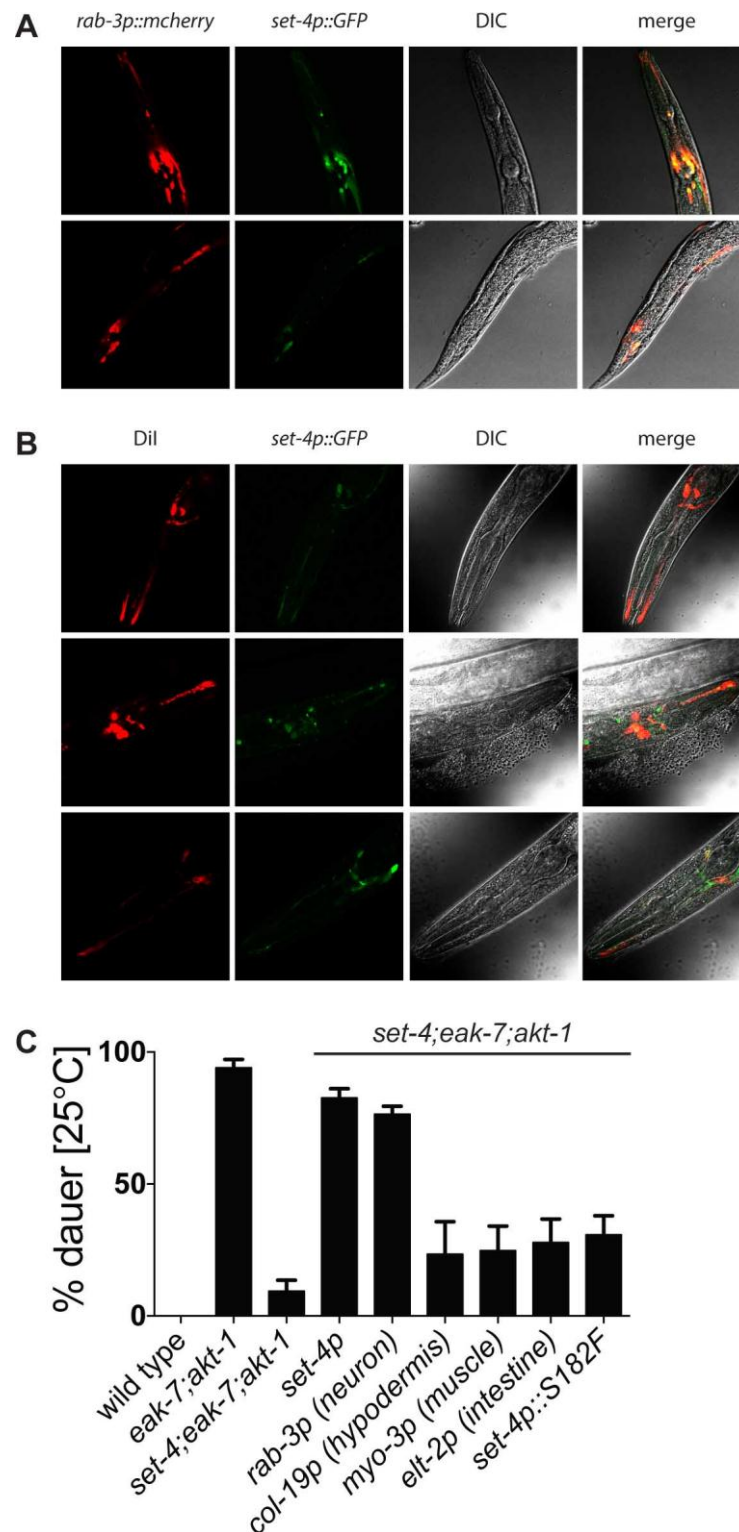
Figure 3. *set-4* acts in the nervous system to promote dauer arrest. (**A**) Representative photomicrographs showing colocalization of GFP and mCherry in animals coexpressing *set-4p::gfp* and the pan-neuronal reporter *rab-3p::mcherry* (N = 15). (**B**) Representative photomicrographs showing colocalization of red and green fluorescence in amphid neurons of *set-4p::gfp* transgenic animals exposed to DiI (N = 21). (**C**) Rescue of dauer arrest in *set-*

4;eak-7;akt-1 mutants by *set-4* transgenes driven by native *set-4* or tissue-specific promoters (N = 2328, 2143, 2058, 662, 811, 705, 936, 516, 541).
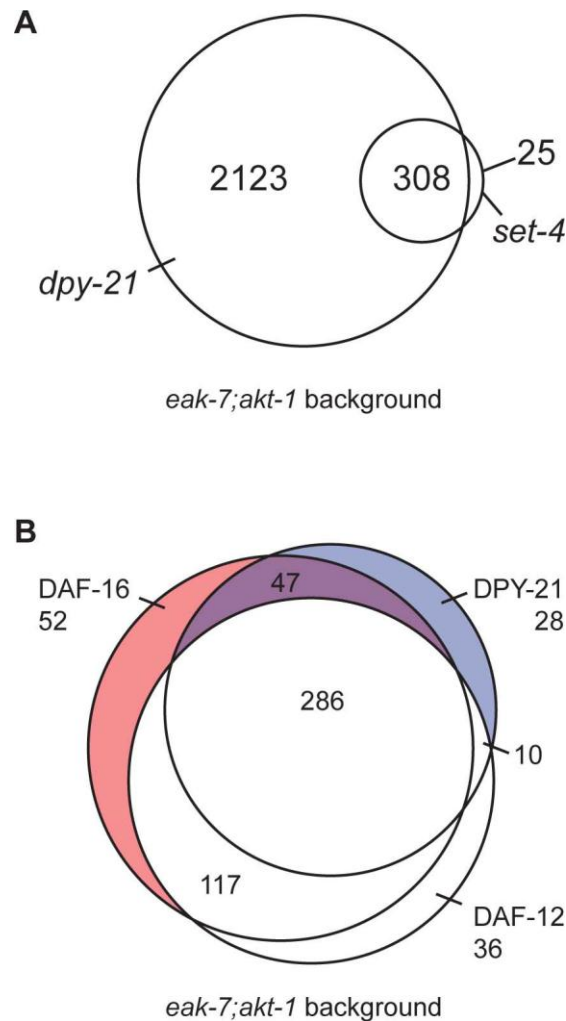
Figure 4. Whole transcriptome profiling defines genes coordinately regulated by DPY-21/SET-4 and DAF-16/FoxO. (**A**) Venn diagram of genes regulated by SET-4 and DPY-21. Genes coordinately regulated by SET-4 and DPY-21 are depicted in gray. (**B**) Venn diagram of X-linked genes regulated by DPY-21, DAF-16/FoxO, and DAF-12. 47 genes coordinately regulated by DPY-21 and DAF-16/FoxO but not by DAF-12 are depicted in purple and listed in Table S5. Data represents the aggregate of five biological replicate samples, each from thousands of progeny of no fewer than 200 animals per sample.
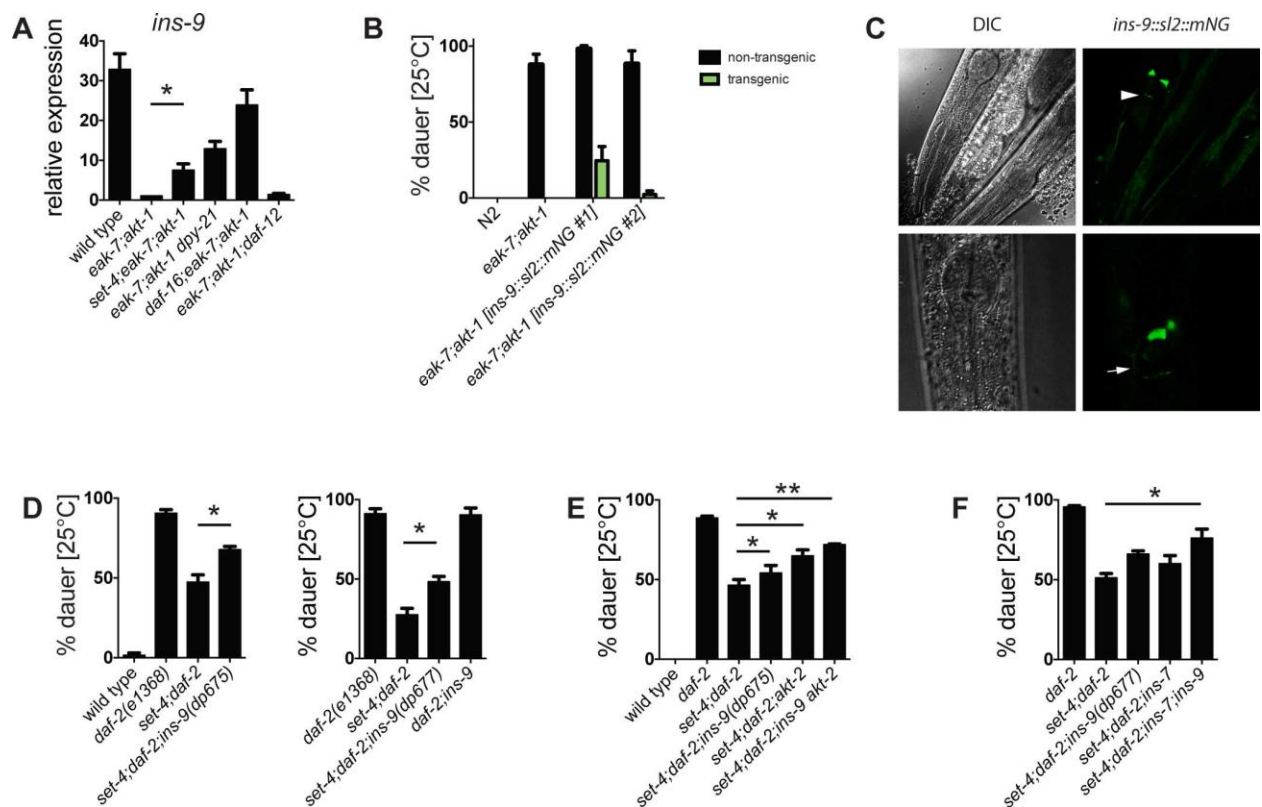
Figure 5. SET-4 promotes dauer arrest by repressing the X-linked *ins-9* gene. (**A**) *ins-9* is repressed by DPY-21, SET-4, and DAF-16/FoxO but not DAF-12. Results are the mean and s.e.m. of five experiments. (**B**) *ins-9* overexpression suppresses dauer arrest in *eak-7;akt-1* animals. Non-transgenic (NT) and transgenic (T) progeny of transgenic hermaphrodites are shown. N = 1200, 1522, 718/156 (NT/T), 702/210 (NT/T). (**C**) An *ins-9::SL2::mNG* transgene is expressed specifically in ASI sensory neurons. The arrowhead indicates the top of the nerve ring, and the arrow indicates the ASI axon. Representative images are shown (N = 20). (**D**) Two *ins-9* nonsense mutations partially rescue dauer arrest in *set-4;daf-2* mutants. N = 957, 1205, 1398 (left panel); N = 892, 1028, 897 (right panel). (**E**) *ins-9* and *akt-2* mutations rescue dauer arrest in an additive fashion in *set-4;daf-2* mutants (N = 949, 1281, 1334, 1524, 1333, 1478) (**F**) *ins-9* and *ins-7* mutations rescue dauer arrest in an additive fashion in *set-4;daf-2* mutants (N = 1396, 1251, 754, 827, 1327). *p<0.05, **p<0.01.
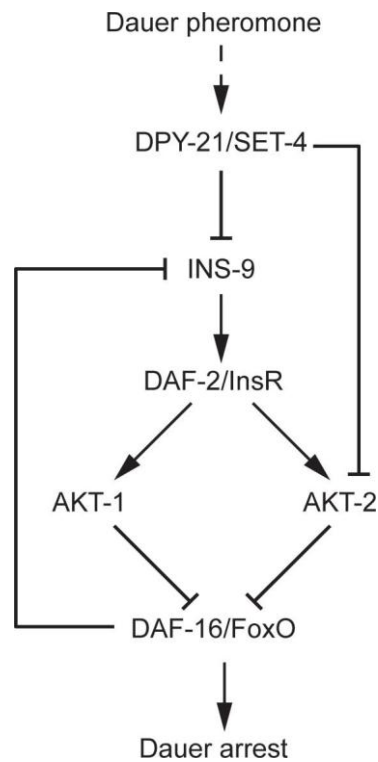
Figure 6. Hypothetical model of dauer regulation by pheromone through DPY-21/SET-4 and DAF-2 ILS. DPY-21 and SET-4 act in concert to promote transduction of pheromone cues by repressing X-linked genes encoding the DAF-2/InsR agonist INS-9 and the serine/threonine kinase AKT-2, resulting in increased DAF-16 activation and subsequent dauer arrest.

SUPPLEMENTARY MATERIALS AND METHODS

Strains

The following mutant alleles were used: *eak-7(tm3188)* (Alam et al., 2010), *akt-1(ok525)* (Hertweck et al., 2004), *set-4(n4600)* (Andersen and Horvitz, 2007), *set-4(ok1481)*, *daf-2(e1368)* (Kimura et al., 1997), *daf-1(m40)* (Georgi et al., 1990), *daf-9(dh6)* (Gerisch et al., 2001), *dpy-21(e428)* (Yonker and Meyer, 2003), *daf-16(mu86)* (Lin et al., 1997), *daf-12(rh61rh411)* (Antebi et al., 2000), *akt-2(ok393)* (Hertweck et al., 2004), *ins-7(tm1907)* (Murphy et al., 2007), *daf-8(e1393)* ((Park et al., 2010), and *daf-36(k114)* (Rottiers et al., 2006). *set-4(n4600)* and *set-4(ok1481)* were a gift from Gyorgyi Csankovszki.

Reporter constructs and transgenic strains

DNA fragments were amplified and assembled using overlap PCR, and fusion products were cloned into pCRXL-TOPO (Invitrogen). GFP, mCherry, and mNeonGreen were amplified from pPD95.75, pSA120, and pDD268, respectively. The identities of fusion products were verified by Sanger sequencing. To generate the single-copy rescuing transgenic strain *dpSi5*, the 638 bp genomic fragment between *set-4* and the upstream gene C32D5.6 (*set-4p*) was amplified and fused to sequence encoding a HA epitope tag followed by the *set-4* open reading frame (*HA::set-4*) and 350 bp of genomic DNA downstream of *set-4* (*set-4utr*) to create *set-4p::HA::set-4::set-4utr*. Single-copy mosSCI integration of *set-4p::HA::set-4::set-4utr* into strain EG6250 (*cxTi10882*) was performed by Knudra Transgenics as described (Frokjaer-Jensen et al., 2008). The *set-4p::GFP* transcriptional reporter was generated by fusing *set-4p* to GFP and *set-4utr* to create *set-4p::GFP::set-4utr*. *set-4p::GFP::set-4utr* was mixed with 50 ng μL^{-1} *rol-6(su1006)* (pRF4) or 10 ng μL^{-1} *rab-3p::mcherry::unc-54utr* to a final DNA concentration of 100 ng μL^{-1} or 50 ng μL^{-1}, respectively. For tissue-specific rescue experiments, promoters defined by the Promoterome Project (worfdb.dfci.harvard.edu/promoteromedb) were amplified from wild-type genomic DNA and fused to *HA:set-4:set-4utr*. The sizes of promoter fragments amplified were as follows: *set-4p*: 638 bp; *rab-3p*: 4913bp; *col-19p*: 1321 bp; *myo-3p*: 2006 bp; *elt-2p*: 1988 bp. Constructs were co-injected with *myo-2p::mcherry::unc-54utr* (pJK343) and

pBlueScript at concentrations of 5, 2, and 43 ng μL^{-1}, respectively. To generate the polycistronic *ins-9::SL2::mNG* transgene, a 1939 bp genomic fragment upstream of *ins-9* was fused to *ins-9* and the intercistronic genomic fragment between *gpd-2* and *gpd-3*, mNeonGreen, and a 1017 bp genomic fragment downstream of *ins-9*. 40 ng μL^{-1} *ins-9::SL2::mNG* was mixed with 10 ng μL^{-1} *rab-3p::mcherry::unc-54utr*. Animals were injected as previously described (Mello et al., 1991) using a Leica DMI3000B microscope and Eppendorf FemtoJet pump.

Antibodies

For immunoblotting, both custom anti-SET-4 antisera, generated by immunizing rabbits with a C-terminal SET-4 peptide (NH_3-ENAEPIISEKKTKYELRSRS-COOH) (Pierce), and anti-H4K20me3 antibodies (Abcam #ab78517) were diluted 1:500. Anti-H4K20me2 antibodies (Abcam #ab9052) and anti-histone H3 antibodies (Abcam #ab12079) were diluted 1:2000 and 1:1000, respectively. The specificity of anti-H4K20me2 and anti-H4K20me3 antibodies was verified using competitive peptide-binding arrays. Methodology and results are available at *www.histoneantibodies.com*.

Dauer pheromone preparation

Wild-type animals were washed into a 2.8L Fernbach flask containing 1L S medium to which 25mL of 40X *E. coli* HB101 culture was added. After media clarified, another 25mL of 40X HB101 was added. Four days later, supernatant was filtered through a Buchner funnel, then vacuum filtered through 0.22 μm SteriTop units (Millipore). Clarified supernatant was evaporated to dryness using a V-10 evaporator (Biotage). Solids were extracted three times with 100 mL 100% ethanol, then evaporated. Pheromone was resuspended in ethanol and effective doses determined empirically. 3.5 cm plates containing 2 mL NGM made with Noble Agar (BD) and lacking peptone were treated with 500 μL water containing the indicated volume of pheromone. Once dry, plates were seeded with 20 μL of 6X *E. coli* OP50 in S basal. Dauer assays were performed as above with animals scored after 84 hr at 25°C.

A

```
C. elegans     SET-4      169-DEDSILAQEGSDFSVMYSTRKRCSTLWLGPAAFINHDCKPNCKFV
D. melanogaster Hmt4-20    297-EEAALLHSGKNDFSVMYSCRKNCAQLWLGPAAYINHDCRANCKFL
H. sapiens     suv420H1    239-EENMLLRHGENDFSVMYSTRKNCAQLWLGPAAFINHDCRPNCKFV
M. musculus    suv420H2    149-DEDLLRAGE-NDFSIMYSTRKRSAQLWLGPAAFINHDCKPNCKFV
S. pombe       Set9        255-EERNIGI--GKDFSILHSSRLDSMCLFLGPARFVNHDCNANCRFN
```
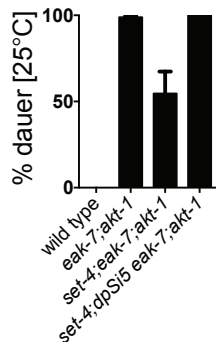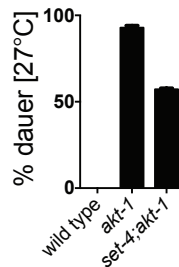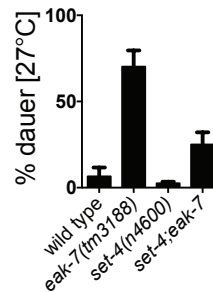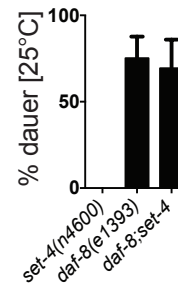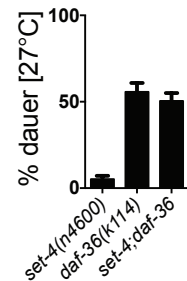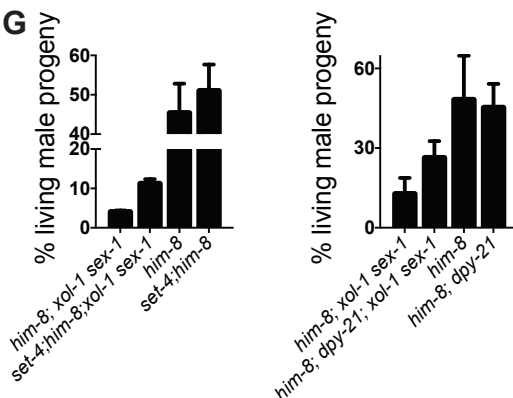

Figure S1. SET-4 promotes dauer arrest and participates in dosage compensation.
(**A**) Conservation of SET-4 serine 182 within the SET domain. Identical and conserved
residues are denoted by black and gray shading, respectively. SET-4 serine 182 is
denoted by the arrow. (**B**) The single-copy *set-4* transgene *dpSi5* rescues dauer arrest in
set-4;eak-7;akt-1 animals (N = 720, 1555, 1096, 1351). *set-4* mutation partially
suppresses the 27°C dauer-constitutive phenotype of (**C**) *akt-1* (N = 806, 1077, 1121) and
(**D**) *eak-7* mutants (N = 409, 472, 379, 318). *set-4* is dispensable for dauer arrest in (**E**)
daf-8 (N = 609, 530, 496) and (**F**) *daf-36* mutants (N = 653, 247, 242). (**G**) *set-4* (N =
4052, 3475, 4486, 3845) and *dpy-21* (N = 3383, 1886, 4171, 3441) mutations rescue
viability of *him-8;xol-1 sex-1* mutant males. Data are representative of three biological
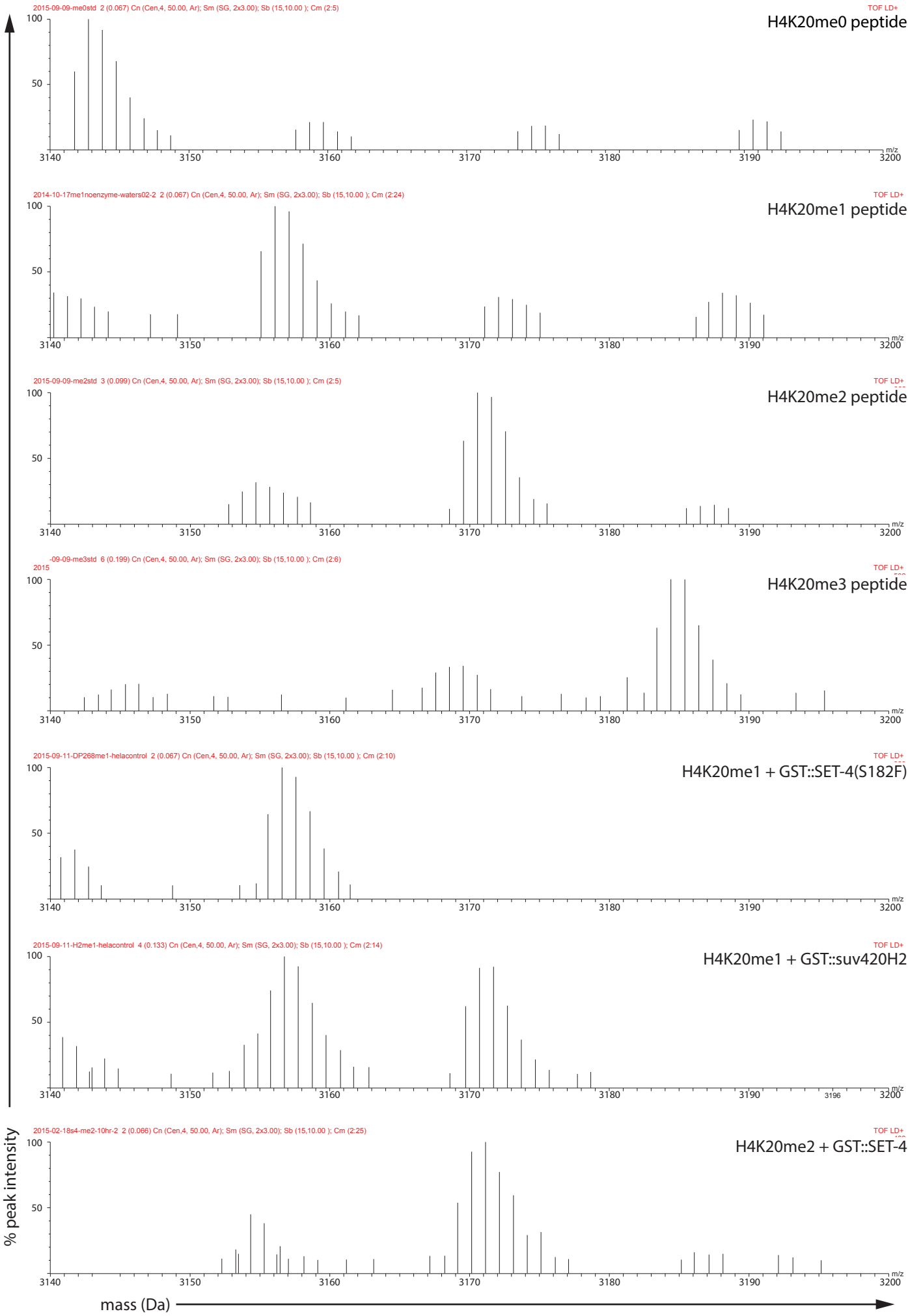replicates.

Figure S2. **MALDI spectra of methyltransferase assays**. Peptide substrates and GST fusion proteins (if any) are indicated. Data are representative of three independent experiments.
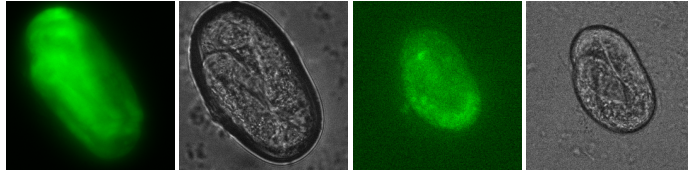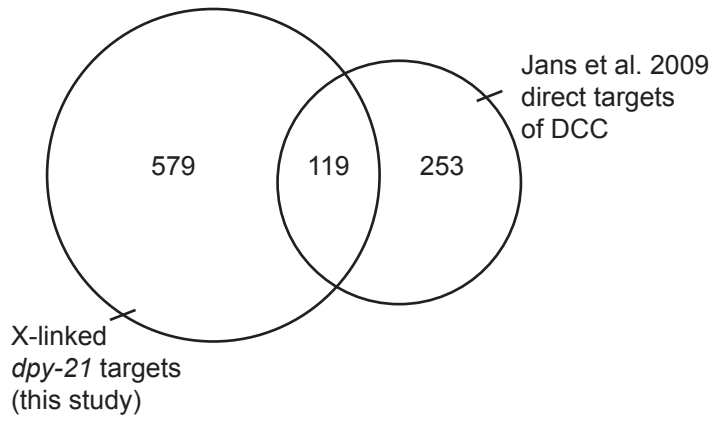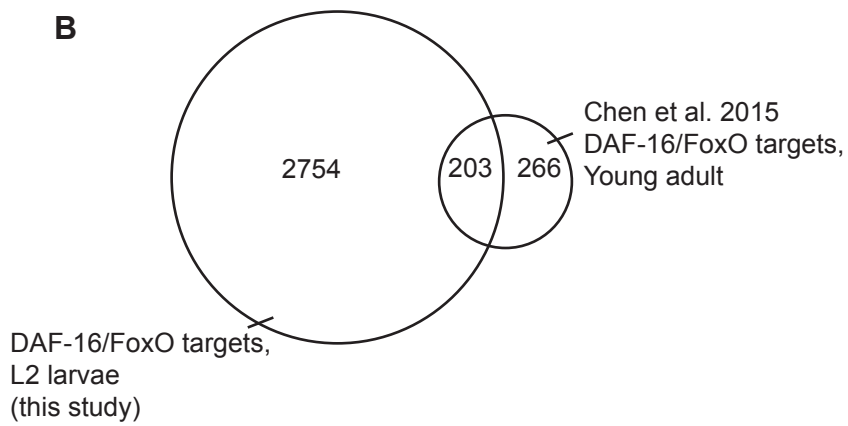
Figure S3. *set-4p::gfp* **expression in embryos.** Embryos from 3 independent transgenic lines were picked from plates and subjected to Nomarski and fluorescent imaging using an Olympus BX61 epifluorescence compound microscope outfitted with a Hamamatsu ORCA ER camera and Slidebook 4.0.1 software. Representative images shown. N = 10.

A

579　119　253

Jans et al. 2009
direct targets
of DCC

X-linked
dpy-21 targets
(this study)

B

2754　203　266

Chen et al. 2015
DAF-16/FoxO targets,
Young adult

DAF-16/FoxO targets,
L2 larvae
(this study)

C

2435　522　594

Liu et al. 2004
SRDG

DAF-16/FoxO targets
(this study)

D

2892　65　67

Liu et al. 2004
DAF-16/FoxO
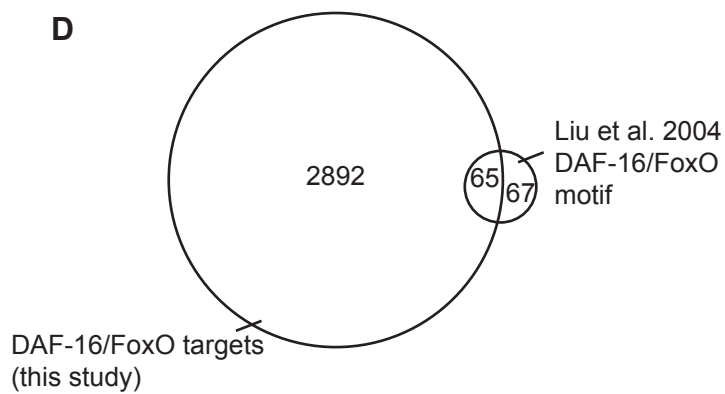motif

DAF-16/FoxO targets
(this study)

Figure S4. **Comparison of whole transcriptome profiling results from this study to published studies.** Venn diagrams depicting significant overlap between (**A**) X-linked genes regulated by *dpy-21* and direct DCC targets (Jans et al., 2009) (overlapping genes listed in Table S2); (**B**) DAF-16/FoxO target genes in L2 larvae and in young adult animals (Chen et al., 2015) (overlapping genes listed in Table S3); (**C**) DAF-16/FoxO target genes in L2 larvae and "strongly regulated dauer genes" (SRDG) (Liu et al., 2004) (overlapping genes listed in Table S4); and (**D**) DAF-16/FoxO target genes in L2 larvae and SRDG containing upstream DAF-16/FoxO binding motifs (Liu et al., 2004) (overlapping genes listed in Table S4).
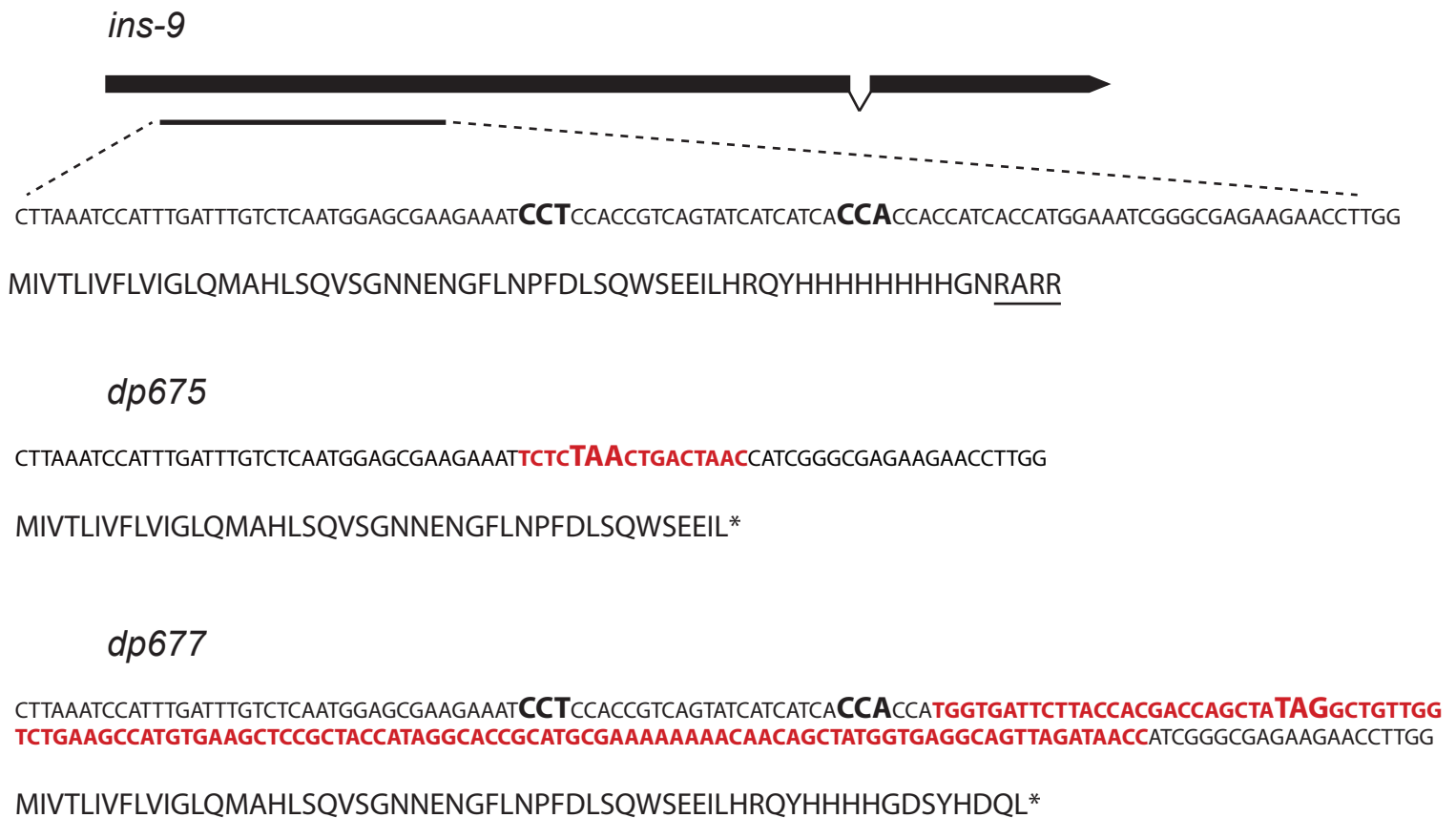
ins-9

CTTAAATCCATTTGATTTGTCTCAATGGAGCGAAGAAAT**CCT**CCACCGTCAGTATCATCATCA**CCA**CCACCATCACCATGGAAATCGGGCGAGAAGAACCTTGG

MIVTLIVFLVIGLQMAHLSQVSGNNENGFLNPFDLSQWSEEILHRQYHHHHHHHHGN<u>RARR</u>

dp675

CTTAAATCCATTTGATTTGTCTCAATGGAGCGAAGAAAT**TCTCTAACTGACTAAC**CATCGGGCGAGAAGAACCTTGG

MIVTLIVFLVIGLQMAHLSQVSGNNENGFLNPFDLSQWSEEIL*

dp677

CTTAAATCCATTTGATTTGTCTCAATGGAGCGAAGAAAT**CCT**CCACCGTCAGTATCATCATCA**CCA**CCA**TGGTGATTCTTACCACGACCAGCTATAGGCTGTTGG
TCTGAAGCCATGTGAAGCTCCGCTACCATAGGCACCGCATGCGAAAAAAAACAACAGCTATGGTGAGGCAGTTAGATAACC**ATCGGGCGAGAAGAACCTTGG

MIVTLIVFLVIGLQMAHLSQVSGNNENGFLNPFDLSQWSEEILHRQYHHHHGDSYHDQL*

Figure S5. **Schematic of the *ins-9* genomic locus and two mutant alleles generated by CRISPR/Cas9-based genome editing.** Nucleotide sequences encoding wild-type, *dp675,* and *dp677* N-terminal F-peptides and predicted N-terminal protein sequences are shown. Targeted CRISPR/Cas9 PAM sites are indicated in bold enlarged black typeface. The putative RXRR prohormone convertase processing site between the F and B peptides is underlined. Inserted sequences in two mutant alleles are indicated in red bold text, and the resultant in-frame stop codons are shown in red, bold and enlarged typeface.
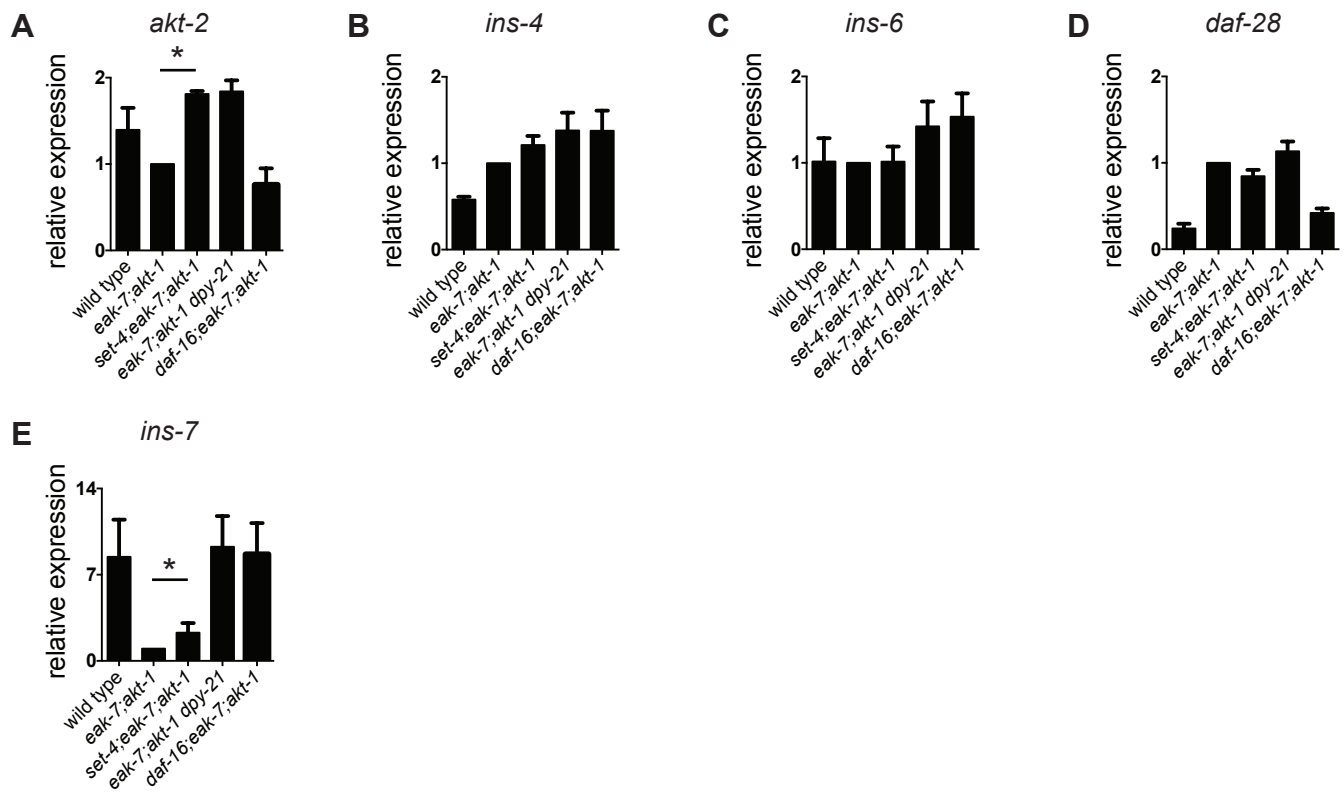
Figure S6. Influence of the DCM and DAF-16/FoxO on the expression of *akt-2* and *ins* genes. Transcript levels of (**A**) *akt-2*, (**B**) *ins-4,* (**C**) *ins-6,* (**D**) *daf-28*, and (**E**) *ins-7* in wild-type and mutant strains. Data presented is the mean plus s.e.m of at least three biological replicates.

Table S1: Lists of genes regulated by DAF-16/FoxO, DAF-12, DPY-21, SET-4, or combinations thereof, based on whole transcriptome profiling. See text for details.

Click here to Download Table S1

Table S2: Subset of DPY-21-regulated X-linked genes that were also previously identified as dosage compensated genes (Jans et al., 2009). See text for details.

Click here to Download Table S2

Table S3: DAF-16/FoxO target genes shared between this study and Chen et al., 2015. See text for details.

Click here to Download Table S3

Table S4: DAF-16/FoxO target genes shared between this study and Liu et al., 2004. See text for details.

Click here to Download Table S4

Table S5: X-linked genes regulated by both DPY-21 and DAF-16/FoxO but not by DAF-12.

Click here to Download Table S5

Table S6: Insulin-like peptide genes regulated by both DAF-16/FoxO and DPY-21.

ILP	chromosome	fold change *daf-16**	fold change *dpy-21!*	*daf-2* interaction
ins-33	I	0.28	0.30	agonist**
ins-29	I	0.54	0.48	?
ins-20	II	2.65	13.32	antagonist@
ins-11	II	2.49	6.69	antagonist@
ins-16	III	0.03	0.07	?
ins-7	IV	10.83	7.99	agonist***
ins-35	V	0.21	0.27	agonist@
ins-9	X	infinite	infinite	agonist#

daf-16;eak-7;akt-1 vs. *eak-7;akt-1*
!*eak-7;akt-1 dpy-21* vs. *eak-7;akt-1*
@Fernandes de Abreu et al, 2014
**Michaelson et al, 2010
***Murphy et al, 2003
#this study

Table S7: CRISPR guide sequences and repair oligonucleotides used for CRISPR/Cas9-based genome editing.

	Sequence 5' to 3'
ins-9 guide #1	GAUGAUGAUACUGACGGUGG
ins-9 guide #2	GAUUUCCAUGGUGAUGGUGG
ins-9 repair oligo	TTCTTAAATCCATTTGATTTGTCTCAATGGAGCGAAGAAATTCTCTAACTGACTAACCATCGGGCGAGAAGAACCTTGGAAACCGAAAAAATCTACCGCT
dpy-10 guide	GCUACCAUAGGCACCACGAG
dpy-10 repair oligo	CACTTGAACTTCAATACGGCAAGATGAGAATGACTGGAAACCGTACCGCATGCGGTGCCTATGGTAGCGGAGCTTCACATGGCTTCAGACCAACAGCCTAT

Table S8: qPCR primer sequences.

Gene		Sequence 5' to 3'
akt-2	F	TCGTGATATGAAACTCGAAAATTTGC
	R	ATTCTGGTGTTCCGCAAAAGGTG
daf-28	F	AGTCCGTGTTCCAGGTGTG
	R	TGTTGCGATGTCAATTCCTT
ins-4	F	AAAATCAACTCTCCCGAGCA
	R	GCAATGTCCATGTCCTCTTGT
ins-6	F	CGAGCAAGACGTGTTCCAG
	R	TCGCAATGTCCTTTCCTTCT
ins-9	F	GAAGAAATCCTCCACCGTCA
	R	GTTCTTCTCGCCCGATTTC
ins-7	F	GTTGTGGAAGAAGAATACATTCGTATG
	R	TCTTCACGGCAACATTTTGATG
pmp-3	F	GTTCCCGTGTTCATCACTCAT
	R	ACACCGTCGAGAAGCTGTAGA

Table S9: Correlation coefficients between experimental replicates and strains analyzed by whole transcriptome profiling.

Click here to Download Table S9

SUPPLEMENTARY MATERIALS AND METHODS

Strains

The following mutant alleles were used: *eak-7(tm3188)* (Alam et al., 2010), *akt-1(ok525)* (Hertweck et al., 2004), *set-4(n4600)* (Andersen and Horvitz, 2007), *set-4(ok1481)*, *daf-2(e1368)* (Kimura et al., 1997), *daf-1(m40)* (Georgi et al., 1990), *daf-9(dh6)* (Gerisch et al., 2001), *dpy-21(e428)* (Yonker and Meyer, 2003), *daf-16(mu86)* (Lin et al., 1997), *daf-12(rh61rh411)* (Antebi et al., 2000), *akt-2(ok393)* (Hertweck et al., 2004), *ins-7(tm1907)* (Murphy et al., 2007), *daf-8(e1393)* ((Park et al., 2010), and *daf-36(k114)* (Rottiers et al., 2006). *set-4(n4600)* and *set-4(ok1481)* were a gift from Gyorgyi Csankovszki.

Reporter constructs and transgenic strains

DNA fragments were amplified and assembled using overlap PCR, and fusion products were cloned into pCRXL-TOPO (Invitrogen). GFP, mCherry, and mNeonGreen were amplified from pPD95.75, pSA120, and pDD268, respectively. The identities of fusion products were verified by Sanger sequencing. To generate the single-copy rescuing transgenic strain *dpSi5*, the 638 bp genomic fragment between *set-4* and the upstream gene C32D5.6 (*set-4p*) was amplified and fused to sequence encoding a HA epitope tag followed by the *set-4* open reading frame (*HA::set-4*) and 350 bp of genomic DNA downstream of *set-4* (*set-4utr*) to create *set-4p::HA::set-4::set-4utr*. Single-copy mosSCI integration of *set-4p::HA::set-4::set-4utr* into strain EG6250 (*cxTi10882*) was performed by Knudra Transgenics as described (Frokjaer-Jensen et al., 2008). The *set-4p::GFP* transcriptional reporter was generated by fusing *set-4p* to GFP and *set-4utr* to create *set-4p::GFP::set-4utr*. *set-4p::GFP::set-4utr* was mixed with 50 ng μL^{-1} *rol-6(su1006)* (pRF4) or 10 ng μL^{-1} *rab-3p::mcherry::unc-54utr* to a final DNA concentration of 100 ng μL^{-1} or 50 ng μL^{-1}, respectively. For tissue-specific rescue experiments, promoters defined by the Promoterome Project (worfdb.dfci.harvard.edu/promoteromedb) were amplified from wild-type genomic DNA and fused to *HA:set-4:set-4utr*. The sizes of promoter fragments amplified were as follows: *set-4p*: 638 bp; *rab-3p*: 4913bp; *col-19p*: 1321 bp; *myo-3p*: 2006 bp; *elt-2p*: 1988 bp. Constructs were co-injected with *myo-2p::mcherry::unc-54utr* (pJK343) and

pBlueScript at concentrations of 5, 2, and 43 ng μL^{-1}, respectively. To generate the polycistronic *ins-9::SL2::mNG* transgene, a 1939 bp genomic fragment upstream of *ins-9* was fused to *ins-9* and the intercistronic genomic fragment between *gpd-2* and *gpd-3*, mNeonGreen, and a 1017 bp genomic fragment downstream of *ins-9*. 40 ng μL^{-1} *ins-9::SL2::mNG* was mixed with 10 ng μL^{-1} *rab-3p::mcherry::unc-54utr*. Animals were injected as previously described ([Mello et al., 1991](#)) using a Leica DMI3000B microscope and Eppendorf FemtoJet pump.

Antibodies

For immunoblotting, both custom anti-SET-4 antisera, generated by immunizing rabbits with a C-terminal SET-4 peptide (NH_3-ENAEPIISEKKTKYELRSRS-COOH) (Pierce), and anti-H4K20me3 antibodies (Abcam #ab78517) were diluted 1:500. Anti-H4K20me2 antibodies (Abcam #ab9052) and anti-histone H3 antibodies (Abcam #ab12079) were diluted 1:2000 and 1:1000, respectively. The specificity of anti-H4K20me2 and anti-H4K20me3 antibodies was verified using competitive peptide-binding arrays. Methodology and results are available at *www.histoneantibodies.com*.

Dauer pheromone preparation

Wild-type animals were washed into a 2.8L Fernbach flask containing 1L S medium to which 25mL of 40X *E. coli* HB101 culture was added. After media clarified, another 25mL of 40X HB101 was added. Four days later, supernatant was filtered through a Buchner funnel, then vacuum filtered through 0.22 μm SteriTop units (Millipore). Clarified supernatant was evaporated to dryness using a V-10 evaporator (Biotage). Solids were extracted three times with 100 mL 100% ethanol, then evaporated. Pheromone was resuspended in ethanol and effective doses determined empirically. 3.5 cm plates containing 2 mL NGM made with Noble Agar (BD) and lacking peptone were treated with 500 μL water containing the indicated volume of pheromone. Once dry, plates were seeded with 20 μL of 6X *E. coli* OP50 in S basal. Dauer assays were performed as above with animals scored after 84 hr at 25°C.

A

```
C. elegans      SET-4      169-DEDSILAQEGSDFSVMYSTRKRCSTLWLGPAAFINHDCKPNCKFV
D. melanogaster Hmt4-20    297-EEAALLHSGKNDFSVMYSCRKNCAQLWLGPAAYINHDCRANCKFL
H. sapiens      suv420H1   239-EENMLLRHGENDFSVMYSTRKNCAQLWLGPAAFINHDCRPNCKFV
M. musculus     suv420H2   149-DEDLLRAGE-NDFSIMYSTRKRSAQLWLGPAAFINHDCKPNCKFV
S. pombe        Set9       255-EERNIGI--GKDFSILHSSRLDSMCLFLGPARFVNHDCNANCRFN
```
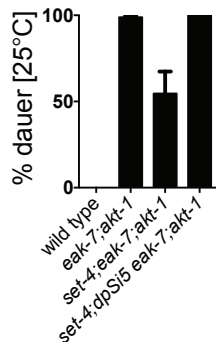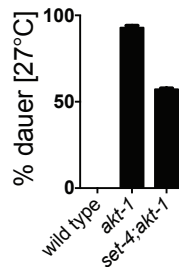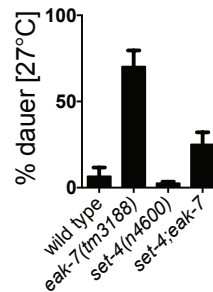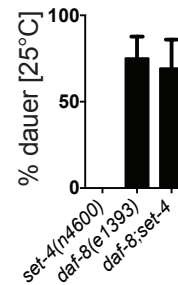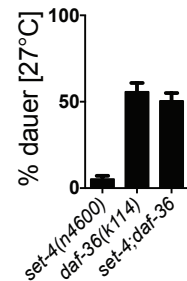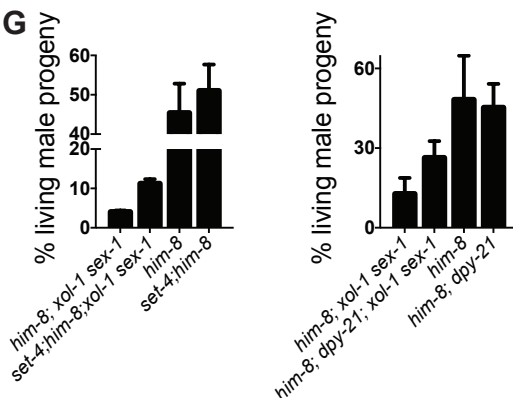

Figure S1. SET-4 promotes dauer arrest and participates in dosage compensation.
(**A**) Conservation of SET-4 serine 182 within the SET domain. Identical and conserved residues are denoted by black and gray shading, respectively. SET-4 serine 182 is denoted by the arrow. (**B**) The single-copy *set-4* transgene *dpSi5* rescues dauer arrest in *set-4;eak-7;akt-1* animals (N = 720, 1555, 1096, 1351). *set-4* mutation partially suppresses the 27°C dauer-constitutive phenotype of (**C**) *akt-1* (N = 806, 1077, 1121) and (**D**) *eak-7* mutants (N = 409, 472, 379, 318). *set-4* is dispensable for dauer arrest in (**E**) *daf-8* (N = 609, 530, 496) and (**F**) *daf-36* mutants (N = 653, 247, 242). (**G**) *set-4* (N = 4052, 3475, 4486, 3845) and *dpy-21* (N = 3383, 1886, 4171, 3441) mutations rescue viability of *him-8;xol-1 sex-1* mutant males. Data are representative of three biological replicates.
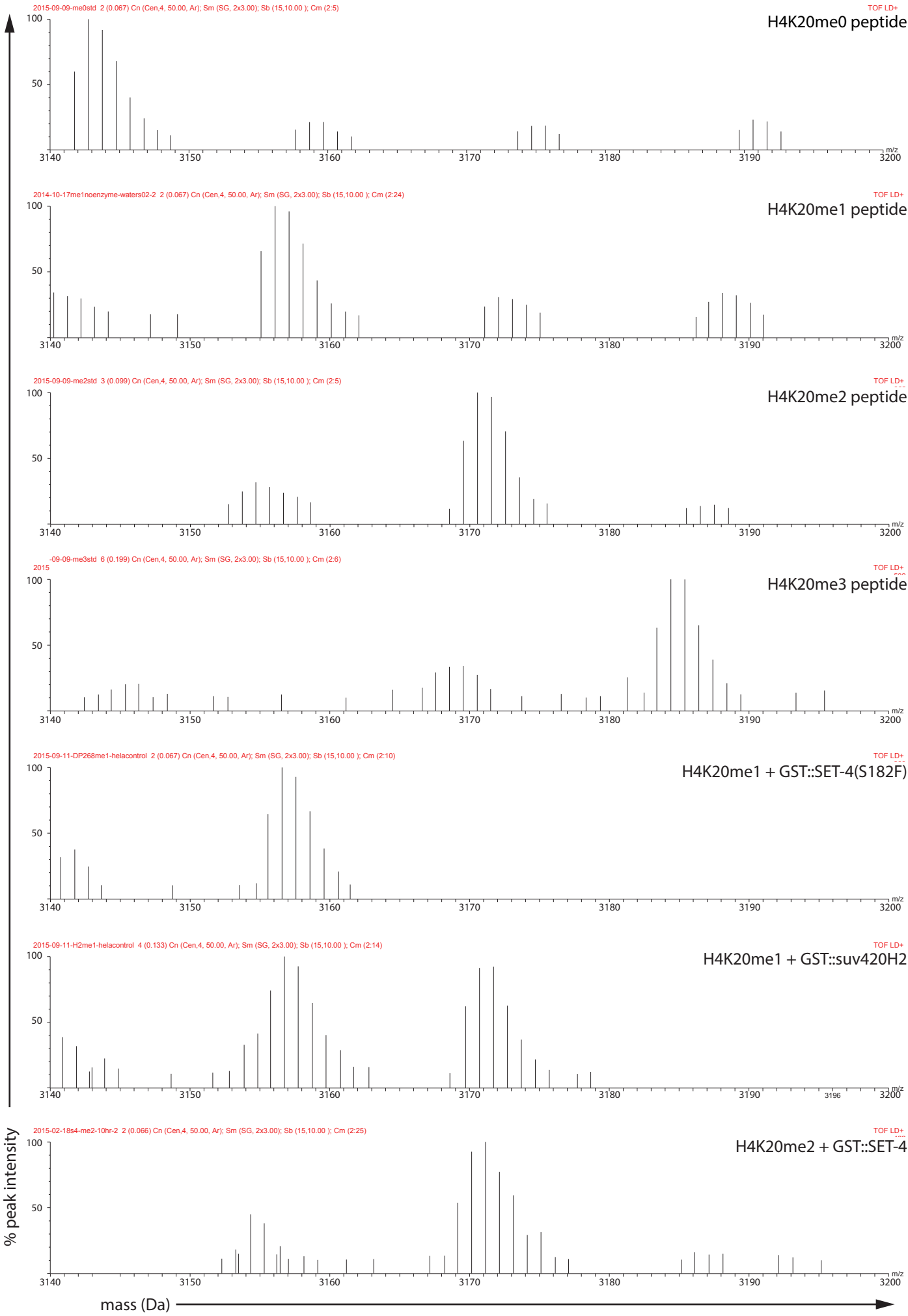
Figure S2. **MALDI spectra of methyltransferase assays**. Peptide substrates and GST fusion proteins (if any) are indicated. Data are representative of three independent experiments.
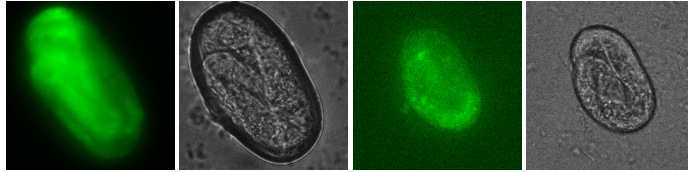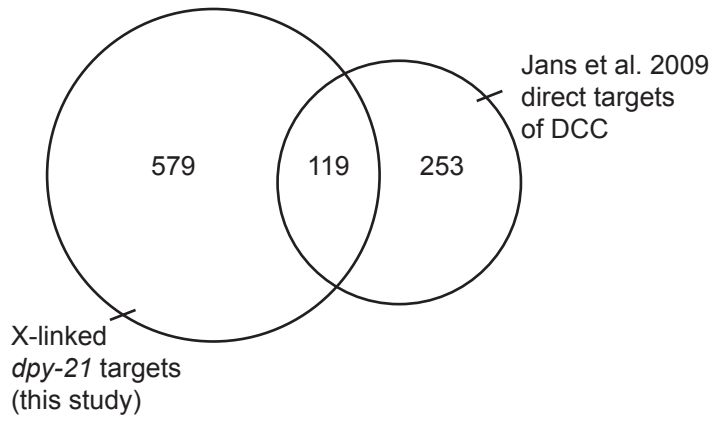
Figure S3. *set-4p::gfp* **expression in embryos.** Embryos from 3 independent transgenic lines were picked from plates and subjected to Nomarski and fluorescent imaging using an Olympus BX61 epifluorescence compound microscope outfitted with a Hamamatsu ORCA ER camera and Slidebook 4.0.1 software. Representative images shown. N = 10.

A

579 119 253

Jans et al. 2009
direct targets
of DCC

X-linked
dpy-21 targets
(this study)

B

2754 203 266

Chen et al. 2015
DAF-16/FoxO targets,
Young adult

DAF-16/FoxO targets,
L2 larvae
(this study)

C

2435 522 594

Liu et al. 2004
SRDG

DAF-16/FoxO targets
(this study)

D

2892 65 67

Liu et al. 2004
DAF-16/FoxO
motif

DAF-16/FoxO targets
(this study)

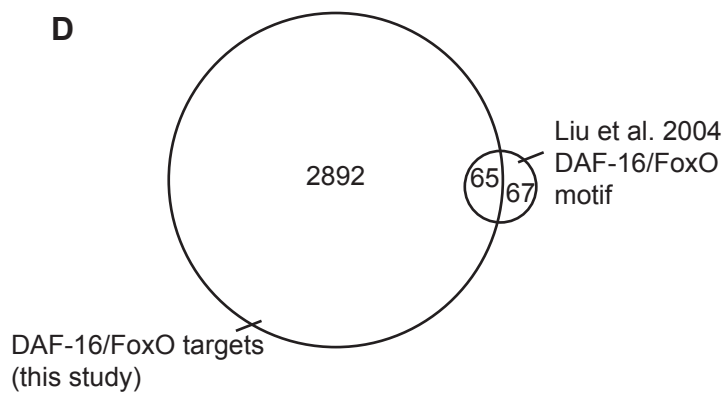**Figure S4**. **Comparison of whole transcriptome profiling results from this study to published studies.** Venn diagrams depicting significant overlap between (**A**) X-linked genes regulated by *dpy-21* and direct DCC targets (Jans et al., 2009) (overlapping genes listed in Table S2); (**B**) DAF-16/FoxO target genes in L2 larvae and in young adult animals (Chen et al., 2015) (overlapping genes listed in Table S3); (**C**) DAF-16/FoxO target genes in L2 larvae and "strongly regulated dauer genes" (SRDG) (Liu et al., 2004) (overlapping genes listed in Table S4); and (**D**) DAF-16/FoxO target genes in L2 larvae and SRDG containing upstream DAF-16/FoxO binding motifs (Liu et al., 2004) (overlapping genes listed in Table S4).
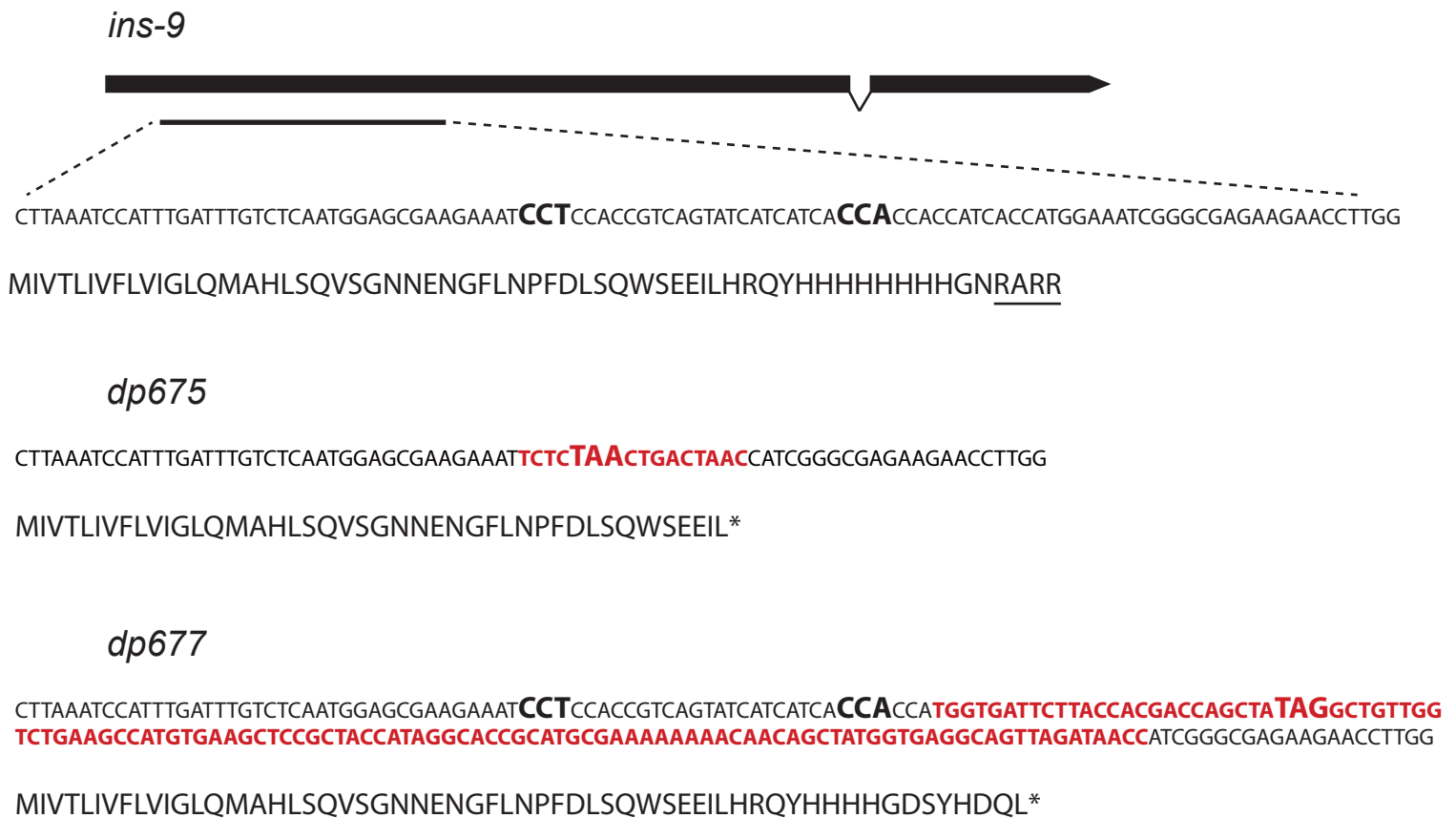
ins-9

CTTAAATCCATTTGATTTGTCTCAATGGAGCGAAGAAAT**CCT**CCACCGTCAGTATCATCATCA**CCA**CCACCATCACCATGGAAATCGGGCGAGAAGAACCTTGG

MIVTLIVFLVIGLQMAHLSQVSGNNENGFLNPFDLSQWSEEILHRQYHHHHHHHHGN<u>RARR</u>

dp675

CTTAAATCCATTTGATTTGTCTCAATGGAGCGAAGAAAT**TCTCTAACTGACTAAC**CATCGGGCGAGAAGAACCTTGG

MIVTLIVFLVIGLQMAHLSQVSGNNENGFLNPFDLSQWSEEIL*

dp677

CTTAAATCCATTTGATTTGTCTCAATGGAGCGAAGAAAT**CCT**CCACCGTCAGTATCATCATCA**CCA**CCA**TGGTGATTCTTACCACGACCAGCTATAGGCTGTTGGTCTGAAGCCATGTGAAGCTCCGCTACCATAGGCACCGCATGCGAAAAAAAACAACAGCTATGGTGAGGCAGTTAGATAACC**ATCGGGCGAGAAGAACCTTGG

MIVTLIVFLVIGLQMAHLSQVSGNNENGFLNPFDLSQWSEEILHRQYHHHHGDSYHDQL*

Figure S5. Schematic of the *ins-9* genomic locus and two mutant alleles generated by CRISPR/Cas9-based genome editing. Nucleotide sequences encoding wild-type, *dp675,* and *dp677* N-terminal F-peptides and predicted N-terminal protein sequences are shown. Targeted CRISPR/Cas9 PAM sites are indicated in bold enlarged black typeface. The putative RXRR prohormone convertase processing site between the F and B peptides is underlined. Inserted sequences in two mutant alleles are indicated in red bold text, and the resultant in-frame stop codons are shown in red, bold and enlarged typeface.
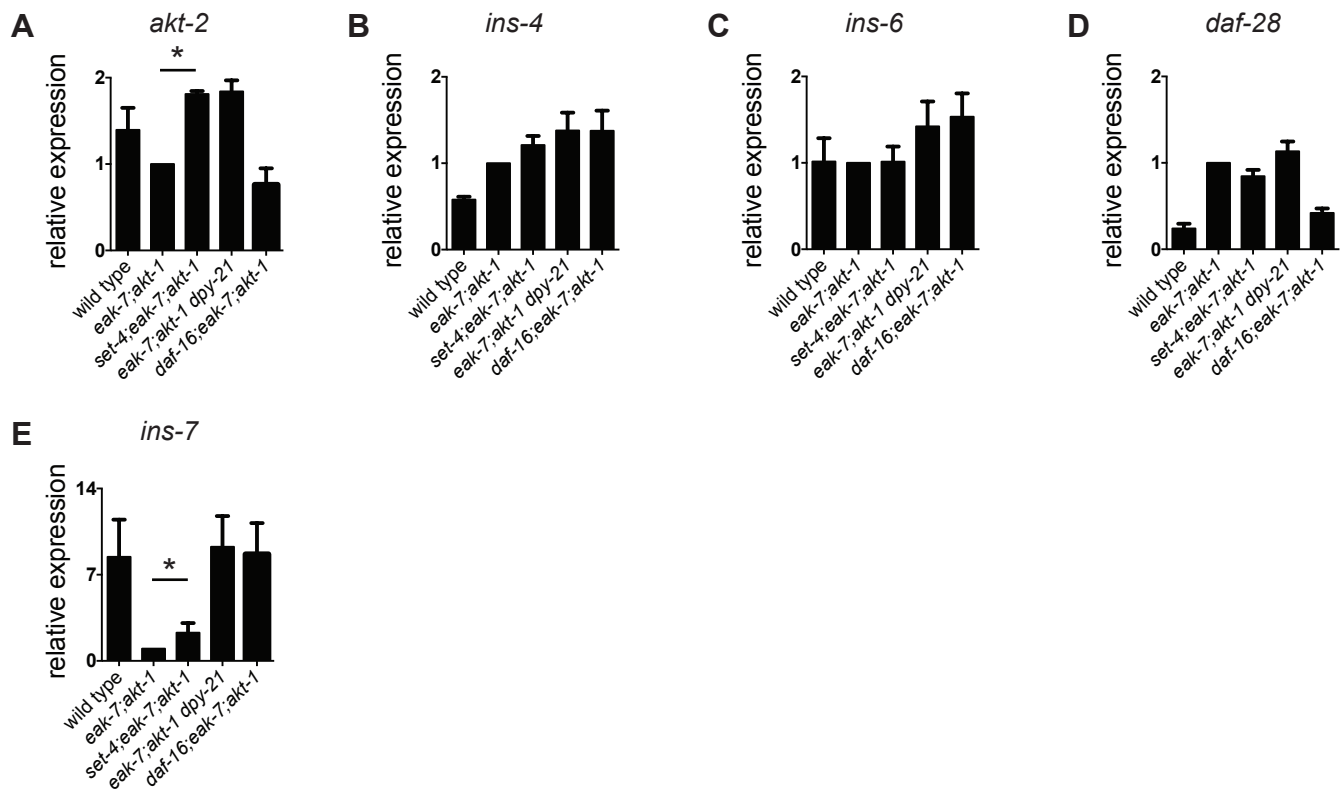
Figure S6. Influence of the DCM and DAF-16/FoxO on the expression of *akt-2* and *ins* genes. Transcript levels of (**A**) *akt-2*, (**B**) *ins-4,* (**C**) *ins-6,* (**D**) *daf-28*, and (**E**) *ins-7* in wild-type and mutant strains. Data presented is the mean plus s.e.m of at least three biological replicates.

Table S1: Lists of genes regulated by DAF-16/FoxO, DAF-12, DPY-21, SET-4, or combinations thereof, based on whole transcriptome profiling. See text for details.

Click here to Download Table S1

Table S2: Subset of DPY-21-regulated X-linked genes that were also previously identified as dosage compensated genes (Jans et al., 2009). See text for details.

Click here to Download Table S2

Table S3: DAF-16/FoxO target genes shared between this study and Chen et al., 2015. See text for details.

Click here to Download Table S3

Table S4: DAF-16/FoxO target genes shared between this study and Liu et al., 2004. See text for details.

Click here to Download Table S4

Table S5: X-linked genes regulated by both DPY-21 and DAF-16/FoxO but not by DAF-12.

Click here to Download Table S5

Table S6: Insulin-like peptide genes regulated by both DAF-16/FoxO and DPY-21.

ILP	chromosome	fold change *daf-16**	fold change *dpy-21ᴵ*	*daf-2* interaction
ins-33	I	0.28	0.30	agonist**
ins-29	I	0.54	0.48	?
ins-20	II	2.65	13.32	antagonist@
ins-11	II	2.49	6.69	antagonist@
ins-16	III	0.03	0.07	?
ins-7	IV	10.83	7.99	agonist***
ins-35	V	0.21	0.27	agonist@
ins-9	X	infinite	infinite	agonist#

daf-16;eak-7;akt-1 vs. *eak-7;akt-1*
ᴵ*eak-7;akt-1 dpy-21* vs. *eak-7;akt-1*
@Fernandes de Abreu et al, 2014
**Michaelson et al, 2010
***Murphy et al, 2003
#this study

Table S7: CRISPR guide sequences and repair oligonucleotides used for CRISPR/Cas9-based genome editing.

	Sequence 5' to 3'
ins-9 guide #1	GAUGAUGAUACUGACGGUGG
ins-9 guide #2	GAUUUCCAUGGUGAUGGUGG
ins-9 repair oligo	TTCTTAAATCCATTTGATTTGTCTCAATGGAGCGAAGAAATTCTCTAACTGACTAACCATCGGGCGAGAAGAACCTTGGAAACCGAAAAAATCTACCGCT
dpy-10 guide	GCUACCAUAGGCACCACGAG
dpy-10 repair oligo	CACTTGAACTTCAATACGGCAAGATGAGAATGACTGGAAACCGTACCGCATGCGGTGCCTATGGTAGCGGAGCTTCACATGGCTTCAGACCAACAGCCTAT

Table S8: qPCR primer sequences.

Gene		Sequence 5' to 3'
akt-2	F	TCGTGATATGAAACTCGAAAATTTGC
	R	ATTCTGGTGTTCCGCAAAAGGTG
daf-28	F	AGTCCGTGTTCCAGGTGTG
	R	TGTTGCGATGTCAATTCCTT
ins-4	F	AAAATCAACTCTCCCGAGCA
	R	GCAATGTCCATGTCCTCTTGT
ins-6	F	CGAGCAAGACGTGTTCCAG
	R	TCGCAATGTCCTTTCCTTCT
ins-9	F	GAAGAAATCCTCCACCGTCA
	R	GTTCTTCTCGCCCGATTTC
ins-7	F	GTTGTGGAAGAAGAATACATTCGTATG
	R	TCTTCACGGCAACATTTTGATG
pmp-3	F	GTTCCCGTGTTCATCACTCAT
	R	ACACCGTCGAGAAGCTGTAGA

Table S9: Correlation coefficients between experimental replicates and strains analyzed by whole transcriptome profiling.

Click here to Download Table S9